

**“Electrical Tuning of Optical Delay in Graphene based Photonic  
Crystal Waveguide”**

Dissertation submitted towards the partial fulfillment of requirement for the award  
of degree of

**Master of Engineering**

**In**

**Electronics and Communication Engineering**

**Submitted by:**

Jobanpreet kaur Thind  
(801361013)

**Under the guidance of:**

Dr. Mukesh Kumar



**ELECTRONICS AND COMMUNICATION ENGINEERING DEPARTMENT**

**THAPAR UNIVERSITY**

**(Established under the section 3 of UGC Act, 1956)**

**PATIALA – 147004 (PUNJAB)**

**June 2015**

## DECLARATION

I, Jobanpreet kaur Thind, hereby declare that the work which is being presented in dissertation entitled "Electrical Tuning of Optical Delay in Graphene based Photonic Crystal Waveguide" is an authentic record of my study carried out as requirement for the award of degree of M.E. (Electronics and Communication Engineering) at Thapar University, Patiala, under the supervision of "Dr. Mukesh Kumar" (Electronics and Communication Engineering department).

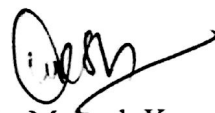
The matter presented in this dissertation has not been submitted in any other university/institute for the award of any other degree.

Date: 29 June, 2015

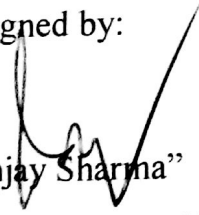
Jobanpreet Kaur Thind  
"Jobanpreet kaur Thind"  
(801361013)


It is certified that the above statement made by the student is correct to the best of my knowledge and belief

Date: 29/06/2015

  
"Dr. Mukesh Kumar"  
"Assistant Professor"  
"ECED"

Countersigned by:

  
"Dr. Sanjay Sharma"  
Professor and Head ECED  
Thapar University, Patiala

  
"Dr. S. S. Bhatia"  
Dean of Academic Affairs  
Thapar University, Patiala

## ACKNOWLEDGEMENT

I would like to express my special thanks and deep special gratitude to my Dissertation Advisor, **Dr. Mukesh Kumar**, Assistant Professor, Electronics & Communication Engineering Department, Thapar University, Patiala for his continuous indefatigable guidance, which paved me on to the path to carry this dissertation. He has always been very encouraging and offered invaluable advice. I am highly indebted to him for his efforts and invaluable suggestions during the period of work.

I am also thankful to our Head of the Department, **Dr. Sanjay Sharma** as well as PG Coordinator, **Dr. Amit Kumar Kohli**, Associate Professor, Electronics and Communication Engineering Department. I would like to thank entire faculty and staff of Electronics and Communication Engineering Department and then friends who devoted their valuable time and helped me in all possible ways towards successful completion of this work. I thank all those who have contributed directly or indirectly to this work.

I wish to express thanks to all those persons who with their encouraging words and suggestions have contributed directly or indirectly for the completion of this work.

## ABSTRACT

Optical signal processing is an efficient and powerful enabler for various communication functions. One of the basic building blocks for achieving efficient and reconfigurable signal processing is a continuously tunable optical delay line. Tunable optical delay lines have various applications in high-performance optical switching and signal processing. The ability to control the group velocity and group delay of slow light can find applications to realize devices for variable delay lines and optical storage and buffering. The purpose of our research is to design and analyze a graphene based photonic crystal waveguide for delay tuning applications. In this dissertation, an electrically controlled graphene based line-defect photonic crystal waveguide is proposed for tuning the group delay. Graphene, a two-dimensional monolayer of carbon atoms, is attracting significant interest due to its unique optical, electrical and chemical properties and its ability to be integrated with existing wave guiding materials such as silicon. It is found that the introduction of few-layer-graphene into photonic crystal waveguide can slow down the guided light. Two designs are proposed: one with graphene on the core region (line-defect) and other with graphene on the cladding region. At telecommunication wavelength 1550 nm, the group delay is tuned from 43 picoseconds to 72 picoseconds in the first design and from 58 picoseconds to 87 picoseconds in the second device design on varying the applied voltage (on graphene) from 1 volt to 4 volts. A group delay tuning of 29 picoseconds is reported with both the designs. Presence of graphene not only provides the way to electrically tune the delay (with low-power) but it also enhances the group delay to some extent. This delay reconfigurability will open up a whole new field of nonlinear signal processing using slow light. The proposed photonic crystal waveguide with graphene can be promising for realization of low-power electrically controllable on-chip delay lines.

# TABLE OF CONTENTS

<b>List of Figures</b>	<b>vii</b>
<b>1. Introduction to Photonic Crystal Waveguide</b>	<b>1</b>
1.1 Fundamentals of Photonic Crystals	1
1.2 Photonic Crystal Slab	3
1.3 Photonic Crystal Waveguide and its Applications	5
1.4 Optical Delay Lines	9
1.5 Applications of Tunable Delay Lines	11
1.5.1 Optical synchronization and multiplexing	12
1.5.2 Optical equalization	12
1.5.3 Optical correlation	12
1.5.4 Optical logic gates	13
1.5.5 Enhanced nonlinear interaction	13
1.6 Purpose and Outline of Thesis	14
<b>2. Graphene based Optoelectronic Devices</b>	<b>15</b>
2.1 Introduction	15
2.2 Applications of Graphene in Optoelectronic devices	20
2.3 Tunable Optoelectronic devices based on Graphene	23
2.4 Use of Graphene for Delay Tuning	27
<b>3. Literature Review</b>	<b>29</b>
<b>4. Electrically Controlled Group Delay in Graphene based Photonic Crystal Waveguide</b>	
4.1 Methodology of Photonic crystal Modeling	39
4.1.1 Wave Equations and Eigen Value Problem	39
4.1.2 Computational Technique – Planewave Expansion method	42
4.2 Design of Proposed Device	43
4.3 Effect of graphene on guiding characteristics	45
4.4 Electrical Control of Graphene	47
	<b>v</b>

4.5 Delay Tuning	49
<b>5. Conclusion and Future Scope</b>	<b>55</b>
5.1 Conclusion	55
5.2 Future Scope	56
<b>References</b>	<b>57</b>
<b>Publications</b>	<b>63</b>

## LIST OF FIGURES

Figure 1.1: Schematic depiction of photonic crystals periodic in one, two, and three dimensions, where the periodicity is in the material structure of the crystal. Only a 3d periodicity can support an omni-directional photonic band gap. 1

Figure 1.2: Band diagrams and photonic band gaps for dielectric rods ( $\epsilon = 12$ ,  $r = 0.2a$ ) in air and air holes ( $r = 0.3a$ ) in dielectric, where 'a' is the lattice constant. The frequencies are plotted around the boundary of the irreducible Brillouin zone. 2

Figure 1.3: Photonic crystal Slab fabricated using Silicon with air holes etched onto it. It helps to realize two dimensional photonic crystal phenomena in three dimensions. 4

Figure 1.4: Projected band diagram for finite-thickness ( $0.5a$ ) slab of air holes in dielectric. The shaded blue region is the light cone: the projection of all states that can radiate in the air. Solid-red/dashed-blue lines denote guided modes (confined to the slab) that are even/odd with respect to the horizontal mirror plane of the slab, whose polarization is TE-like/TM-like, respectively. There is a band gap (region without guided modes) in the TE-like guided modes only. 4

Figure 1.5: Band structure of line-defect formed by removing a row of rods from a perfect square lattice, plotted versus the wave vector component  $k$  along the defect. Extended modes in crystal become continuum regions (blue), whereas inside the band gap (yellow) a defect band (red) is introduced corresponding to a localized state. 5

Figure 1.6: (a) Schematic depiction of a two-dimensional photonic crystal W1 waveguide. (b) Blue line: light line, Green line: Dispersion curve of W1 waveguide mode with: lattice constant 'a' = 420 nm, hole radius 'r' = 125 nm and refractive index  $n = 3.31$ . 6

Figure 1.7: a) Schematic band diagram and group-index spectrum for silicon PCW. b) Schematic band and group-index spectrum of silicon PCW. c) Transmission spectrum, group-index spectrum and band diagram with respect to the normalized frequency for a silicon PCW [8]. 8

Figure 1.8: (a) Tunable delay line structure using microring resonators with overall central frequency  $\omega_r$ . In order to tune the delay, the resonances of the red rings are red shifted by

increasing the refractive index of the ring, while the resonances of blue rings are blue shifted by decreasing the refractive index of the rings. (b) Electrical delay tuning of slow light pulses in pin-diode-incorporated photonic crystal waveguide. 9

Figure 1.9: Cross-correlator using locally heated photonic crystal coupled waveguide and pulse compressor. 12

Figure 2.1: Graphene as 2D material for carbon materials of all dimensionalities. It can be wrapped up into 0D fullerenes, rolled into 1D nano tubes or stacked into 3D graphite. 15

Figure 2.2: Chiral quantum Hall effect (QHE). a) The hallmark of massless Dirac fermions is QHE plateaux in  $\sigma_{xy}$  at half integers of  $4e^2/h$ . b) Anomalous QHE for massive Dirac fermions in bilayer graphene is more subtle (red curve). It exhibits the standard QHE sequence with plateaux at all integer  $N$  of  $4e^2/h$  except for  $N = 0$ . The missing plateau is indicated by the red arrow. The zero- $N$  plateau can be recovered after chemical doping, which shifts the neutrality point to high  $V_g$  so that an asymmetry gap ( $\approx 0.1\text{eV}$ ) is opened by the electric field effect (green curve). 17

Figure 2.3: (a) Band diagram of graphene showing the linear dispersion of the carriers near the Dirac point, where the conduction and the valence band meet. (b) If the Fermi energy is shifted under the application of an electric field, then the light cannot get absorbed in graphene anymore. (c), (d): Real and imaginary part of the refractive index of graphene as a function of the applied gate voltage. 19

Figure 2.4: (a) Schematic of electro-optic modulator device from Liu et al. (b) Transmission of optical signal vs. drive voltage applied to the gold contact pads. There are three distinct regions of operation, which correspond to the shifting of the Fermi level. 20

Figure 2.5: Schematic of graphene waveguides by Kim et al. Graphene strips of length 5.7 mm are patterned between a 20  $\mu\text{m}$ -thick dielectric on both sides. 21

Figure 2.6: Schematic model of fiber-to-graphene coupler based on a side-polished optical fiber; here LG is the propagation distance (length of covered graphene film). 22

Figure 2.7: Ambipolar electric field effect in single-layer graphene. The insets show low-energy spectrum  $E(k)$ , indicating changes in position of Fermi energy  $E_F$  with changing gate

voltage  $V_g$ . Positive (negative)  $V_g$  induces electrons (holes). The rapid decrease in resistivity  $\rho$  on adding charge carriers indicates their high mobility. 23

Figure 2.8: Schematic of the photonic crystal cavity-graphene device. The cavity is fabricated on a silicon-on-insulator platform, and the electrical gating is performed by means of contacts (drain, source, and gate) covered by an ion-gel. 24

Figure 2.9: (a) The band structures of graphene at different doping levels; graphene becomes more transparent when interband transitions are Pauli blocked, as shown in images on the left and right. (b) Schematic of the electrically controlled graphene-Photonic crystal nano-cavity. A thin hafnium oxide ( $\text{HfO}_2$ ) layer is grown on the chip before the graphene transfer to isolate the Si slab and graphene electrically. 25

Figure 2.10: Graphene-based photonic crystal: a) side view. The material of the dielectric between graphene discs can be the same as the material of dielectric substrate b) top view. 26

Figure 4.1: (a) Schema of 2d photonic crystal of hexagonal lattice of air holes in high dielectric material. Unit cell is repeated infinitely along the primitive vectors  $a_1$  and  $a_2$ . Its first Brillouin zone, with high symmetry points, is shown underneath. (b) A two dimensional photonic crystal line-defect waveguide defined by the repetition of a supercell. 40

Figure 4.2: a) Top view and cross sectional view of the graphene based photonic crystal waveguide device design in which graphene layer is placed on the core region (line-defect). b) Top view and cross sectional view of the graphene based photonic crystal waveguide device design in which graphene layer is placed on the cladding region. The basic two dimensional photonic crystal is fabricated made on a SOI platform. On silicon substrate, a layer of  $\text{SiO}_2$  is deposited. Over which top silicon layer is present in which air holes ( $n=1$ ) are etched, which provides the required dielectric contrast. 42

Figure 4.3: Electric field energy density profile of guided mode in graphene based pcw calculated by plane wave expansion method showing band gap guiding effect. 43

Figure 4.4: Group velocity ( $v_g$ ) of the defect guided mode in the waveguide in  $c$  (the speed of light in the vacuum), for the photonic crystal waveguide without the use of graphene. 43

Figure 4.5: Group velocity ( $v_g$ ) of the guided mode in the graphene based photonic crystal

waveguide a) when graphene is placed on the core region (line-defect) b) when graphene is placed on the cladding region. 44

Figure 4.6: Group velocity versus wavelength for photonic crystal waveguide and effect of graphene on core/clad. The inset shows effect of graphene (core/clad) on group index ( $n_g$ ) indicating slow light enhancement. 44

Fig 4.7: The real and imaginary part of the dielectric constant of graphene as a function of the applied gate voltage. The real part is a non-monotonic function of the applied voltage. The imaginary part decreases monotonically with increasing voltage. 46

Figure 4.8: The variation of Group velocity of the guided mode in photonic crystal waveguide with applied electric voltage. Here black line denotes no voltage, blue line indicates 30V and red line indicates group velocity when 50V is applied to the device. 47

Figure 4.9: Tunable Delay (in picoseconds) of the Photonic crystal waveguide without using graphene at 1550nm. This depicts that with increasing voltage, group delay increases. 48

Figure 4.10: The variation of Group velocity of the guided mode in graphene based photonic crystal waveguide with applied electric voltage when graphene is placed on core (line-defect). 48

Figure 4.11: Tunable Delay (in picoseconds) of the graphene based photonic crystal waveguide at 1550nm when graphene is placed on the core region (line-defect). 49

Figure 4.12: The variation of Group velocity of guided mode in graphene based photonic crystal waveguide with applied electric voltage when graphene is placed on the clad (air-holes). 50

Figure 4.13: Tunable Delay (in picoseconds) of the graphene based photonic crystal waveguide at 1550nm when graphene is placed on the clad (region with air-holes). 50

Fig 4.14: Comparison of tuning of group delay by varying applied voltage on graphene (on core/clad) at a wavelength of 1550 nm. The inset shows the delay vs. applied voltage for the PCW without the use of graphene. 51

# CHAPTER 1

## Introduction to Photonic Crystal Waveguide

### 1.1 Fundamentals of Photonic Crystals

Photonic crystals are artificial materials with macroscopic arrangement of periodic modulation of dielectric constant [1]. These are designed with the objective of controlling the optical properties of materials in same way as the crystal structure of semiconductors controls the propagation of electronic waves through it. From semiconductor physics, it is known that a periodic potential can prohibit the propagation of electrons with certain energies and in certain directions, by creating a gap in the energy band structure. Outside the gap, the electrons can propagate freely, but with different properties than the electrons in free space. Photonic crystals are the optical analogue of ordinary crystals and therefore these help in the designing of the materials that perfectly reflect electromagnetic waves in a certain range of frequencies, or allow them to propagate only in one direction, or modify their free-space properties in various other ways. This capability opens up a variety of opportunities for technological developments in high-speed computing, laser physics, and spectroscopy.

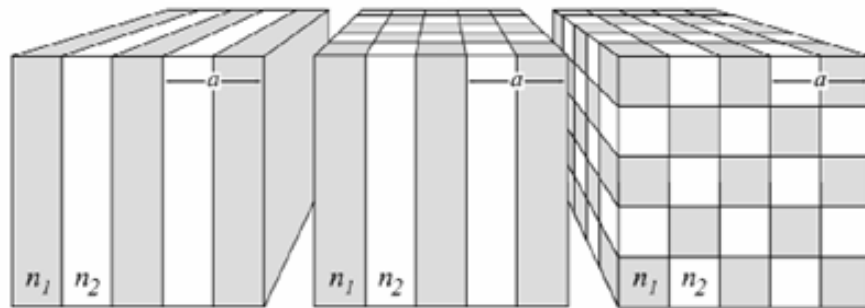


Figure 1.1: Graphic depiction of photonic crystals periodic in one, two, and three dimensions. The periodicity is in the material structure of crystal. Only 3d periodicity supports an omni-directional photonic band gap [2].

The simplest photonic crystal is a periodic stack of layers with different dielectric constants. It is a one-dimensional crystal as it is periodic along one direction and homogeneous along the other two. It was studied first by Lord Rayleigh in 1887. By summing multiple reflections and refractions at each interface he showed that a multilayer film has a band gap. Therefore, such a photonic crystal can serve as a mirror, known as Bragg mirror, and it can confine electromagnetic waves by introducing certain defects in the periodic structure. A two

dimensional photonic crystal is periodic in two directions and homogeneous in the third. In two dimensions the electromagnetic waves decouple into TE modes (electric field in the plane of periodicity) and TM modes (magnetic field in the plane of periodicity). A complete band gap possibly will appear from the interference of refracted and reflected waves. This band gap prohibits the light from propagating in any direction in the plane of periodicity. As a consequence the light modes with a frequency within the band gap can be trapped by point defects in the crystal structure or guided from one location to another by line defects. The complete optical analogue of a conventional crystal is a three dimensional photonic crystal, which is periodic along all three axes. Similar phenomena occur in this case as in the two-dimensional case with the additional possibility to confine electromagnetic radiation in all three dimensions.

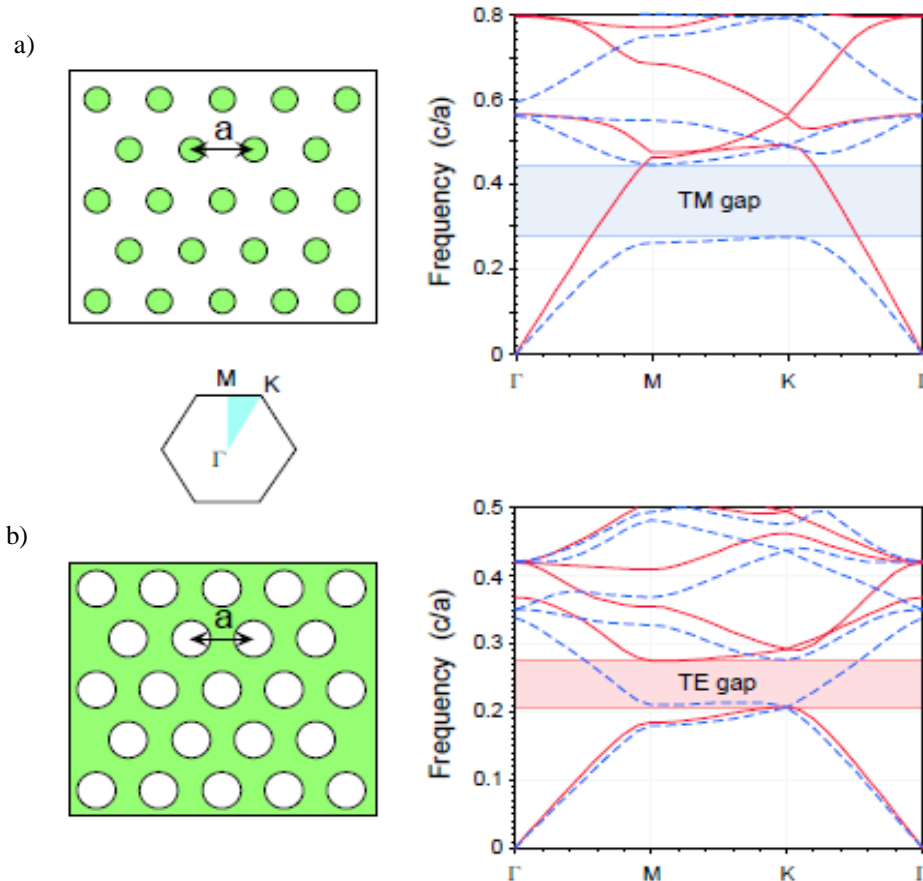


Figure 1.2: Band diagram and photonic band gap. (a) Dielectric rods ( $\epsilon=12$ ,  $r=0.2a$ ) in air. (b) Air holes ( $r=0.3a$ ) in dielectric material. Taking the irreducible Brillouin zone, the frequencies are plotted around its boundary [3].

The two dimensional photonic crystals exhibit most of the important characteristics of photonic crystals, from minimum index contrast to nontrivial Brillouin zones, and can be used to exhibit most of the proposed photonic-crystal devices. The way to understand photonic crystals in two dimensions is to realize that the fields in two-dimension can be divided into two polarizations. First is TM (transverse magnetic), in which the magnetic field is in the (xy) plane and the electric field is perpendicular (z). Second is TE (transverse electric), in which the electric field is in the (xy) plane and the magnetic field is perpendicular (z). Analogous to these two polarizations, there are two structures for two dimensional photonic crystals, as depicted in Figure 1.2: (a) high index rods surrounded by low index which is best suited for TM light and (b) low-index holes in high index which is best suited for TE light. The structure depicted in figure 1.2 (a) provides a large TM band gap and structure shown in (b) figure provides large TE gap. Since Maxwell's equations are scale-invariant [1], therefore same solutions can be used for any wavelength by simply choosing the appropriate lattice constant. Therefore photonic crystals can be constructed to control waves of almost any frequency.

The band diagram for a photonic crystal is a multi-dimensional surface that can be sliced to create dispersion contours. This is an analogy of the Fermi surface in solid state physics. A two-dimensional photonic crystal is actually a three dimensional structure, having symmetry in the two in-plane  $k$  vectors. Therefore its band structure is described by these two  $k$  vectors and the frequency  $\omega$ , thus forming a three-dimensional band contour surface. By intersecting a fixed  $\omega$  frequency plane with the band contour, a dispersion surface or dispersion contour, is created. Multiple equifrequency contour plots can be created by this method, creating a diagram that indicates the allowable wavevectors in the photonic crystal medium. These dispersion contours allow wave vector propagation information to be obtained through the use of  $k$ -vector line constructions.

## 1.2 Photonic Crystal Slab

In order to realize two dimensional photonic crystal phenomena in three dimensions, the most simple design is to fabricate a two dimensional periodic crystal with a finite height, i.e., a photonic-crystal slab. The photonic crystal slab, which has two dimensional in-plane periodicity, is one of the most attractive photonic crystal structures. Such structure can

confine light within the slab vertically via the phenomena of index guiding i.e., generalized total internal reflection. Slabs have two critical parameters that influence the existence of a gap. It must have mirror symmetry so that the gaps in even and odd modes can be separately considered. Also, height of the slab must be optimum. If slab height is too small then the modes are weakly confined and if too large, higher-order modes fill the gap. The optimum slab height is around half a wavelength.

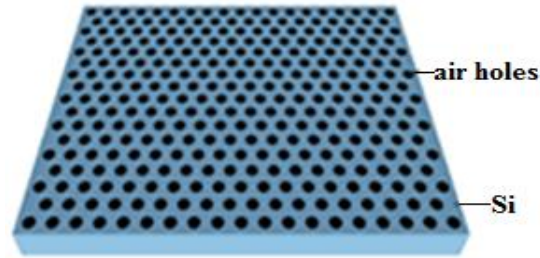


Figure 1.3: Photonic Crystal Slab fabricated using silicon with air holes etched onto it. It helps to realize two dimensional photonic crystal phenomena in three dimensions [4].

The slab is interesting because it is easy to fabricate in comparison to three dimensional photonic crystals and also has manageable chip-level integration. Slab has high refractive index material, acting as core, which is encompassed by lower refractive index material that acts as cladding. This allows confinement of light in the z-direction through index guiding. These have properties different from 2d photonic crystals having infinite height.

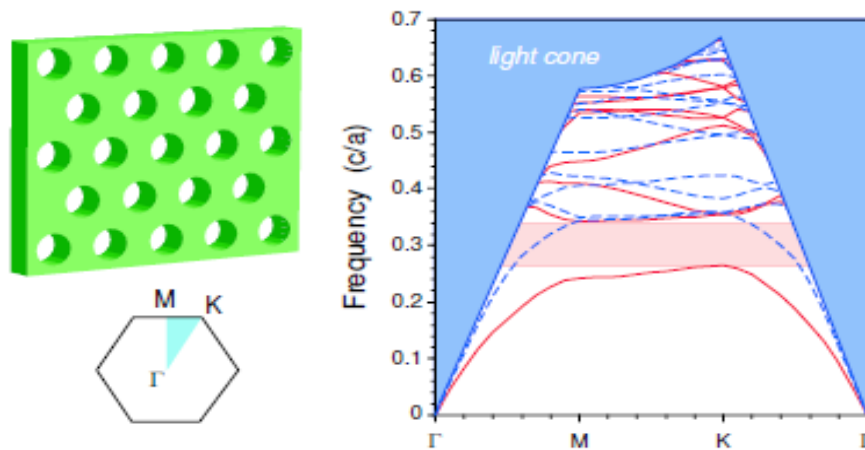


Figure 1.4: Projected band diagram for finite-thickness ( $0.5a$ ) slab of air holes in dielectric. Blue region depicts the light cone: it projects all states that radiate in air. Red/Blue lines depict the guided modes, which are confined to slab, with polarization TE/TM and that are even/odd w.r.t. horizontal mirror plane of slab, respectively. In this structure, a photonic band gap, i.e., region without guided modes exists in the TE guided modes [4].

In 2d photonic crystals Eigen modes are TE and TM modes but not in photonic slabs because of the finite height property associated. When both the claddings are identical to each other and middle of slab offers symmetry, Eigen modes of slab can be categorized into even and odd modes. Field distribution pattern of magnetic component in z-direction become symmetrical for even modes and asymmetrical for odd modes. In case of first order modes polarization mixing is very acute and can be taken as odd TM-like polarized and even TE-like polarized. Another significant difference is behavior of the light line that consists of radiation modes extending infinitely in areas outside slab. Localization of guided modes to slab may only exist within regions of band diagram which are out of light cone. The modes lie inside region of leaky modes of planar waveguide specifically for above light line of the cladding material. These have intrinsic radiation losses associated to out-of-plane diffraction and called quasi-guided modes. Below light cone the discrete bands are the guided modes.

### 1.3 Photonic Crystal Waveguide and its Applications

A Photonic crystal waveguide consists of a line-defect introduced in a photonic crystal, which disturbs the periodicity of the structure. It is introduced by removing air holes from photonic crystal slab fabricated using silicon. Light propagates in the photonic crystal structure through the defect. It propagates in the vertical direction through total internal reflection and in the lateral direction through Bragg reflection, which occurs due to the photonic band gap. Slow light is generated in the region near the photonic band edge due to the effect of strong dispersion in the line-defect [5].

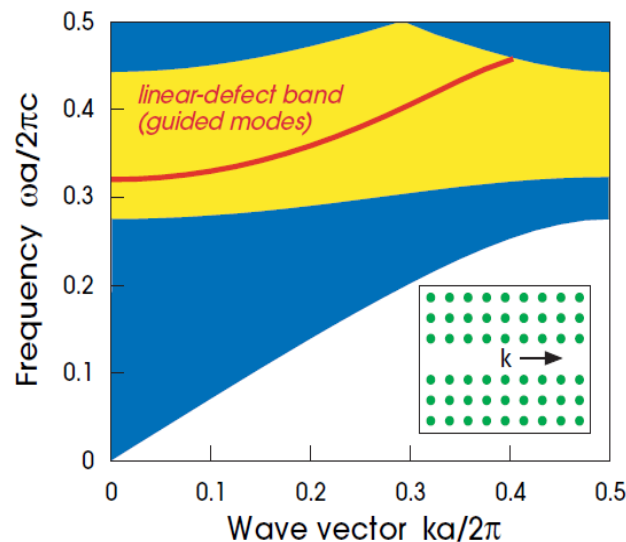


Figure 1.5: Band structure of line-defect formed by removing a row of rods from a perfect square lattice, plotted versus the wave vector component  $k$  along the defect. Extended modes in crystal become continuum regions (blue), whereas inside band gap (yellow) a defect band (red) is introduced corresponding to a localized state [1].

The existence of two-dimensional gap allows us to design a waveguide by forming linear defect in the crystal. To obtain a guided mode propagating within the crystal structure in a certain direction, defects should be introduced. In this way, light wave can be captured in defects and propagation to adjoining places is inhibited. If these defects are continuously formed in a certain direction, a photonic crystal waveguide is formed. A range of frequencies occupying the band gap of the regular photonic crystal structure can propagate in this line-defect waveguide in a specific direction. We can remove a single row of rods from the crystal, resulting in guided mode shown in figure 1.5. Also shown is projected band diagram, the guided mode (red, in yellow-shaded gap) covers range of frequencies described by its dispersion relation. A feature of this waveguide is that light is guided primarily within air, much like a hollow metallic waveguide, but unlike traditional index-guiding structure. This property can be exploited to reduce the interaction between light and the material in order to reduce absorption or nonlinearities [6].

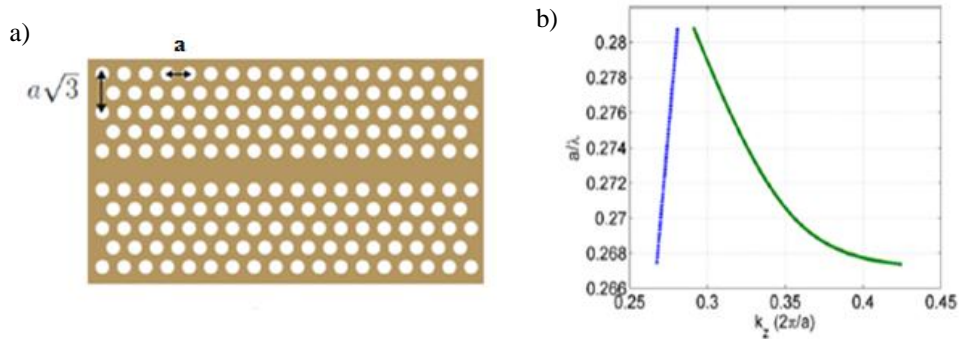


Figure 1.6: (a) Schematic depiction of a two-dimensional photonic crystal W1 waveguide. (b) Blue line: light line, Green line: Dispersion curve of W1 waveguide mode with: lattice constant  $a=420$  nm, hole radius  $r=125$  nm and refractive index  $n=3.31$ [7].

Photonic crystal waveguides where just one line of holes is missing are called W1 waveguides. Figure 1.6 (a) shows a W1 waveguide. Variations can be made to build different kinds of waveguides following the same principle. These waveguides can be either mono or multimode. A small thickness of slab ensures monomode operation. Figure 1.6 (b) shows the dispersion curve of mode propagation in W1 photonic crystal waveguide with a triangular lattice period  $a=420$ nm, refractive index  $n=3.31$ , and hole radius  $r=125$  nm.

The group velocity ( $v_g$ ) is the derivative of frequency with respect to the wave vector, i.e. the slope of the dispersion curve. Figure 1.6.b shows that as we approach the limit of the Brillouin zone, the group velocity becomes smaller and thus the corresponding group index ( $n_g$ ) is large. A large group index value denotes large slowdown in the speed of light propagating through the photonic crystal waveguide which is highly advantageous for on-chip slow light applications. The photonic crystal line-defect waveguide allows ultra small components and low group velocity  $v_g$  [8] due to its strong optical confinement by the photonic band gap. The abrupt discontinuity in the density of photon states near a photonic band gap enables the study of numerous interesting physical phenomena. Investigation into 2d waveguides has mostly been focused on numerical modeling or novel mathematical formalisms such as Winner function expansions and analytical solutions. These approaches are now used to tackle more application-based problems, such as single-mode versus multi-mode design and the existence of non-propagating bound states in waveguides. Advantage of photonic crystal waveguides over their conventional dielectric counterparts is their ability to confine light even at sharp bends. Work on bent waveguides has been mostly restricted to two dimensional crystal structures due to the computational requirements for the three dimensional structures.

Photonic crystal waveguides are the most common commercial products that involve two dimensional periodic photonic crystals using a micro-scale structure to confine light with radically different characteristics compared to conventional optical fiber and waveguides for potential applications in guiding extraordinary wavelengths and non-aligned devices. In the next generation networks, path switching of packets of optical data at the nodes of the network becomes vital and solutions that can perform this task with high data rate, low power consumption and high throughput are needed. All optical processing based photonic routers [9] are being developed which avoids conversion to electrical domain and thus reduces inefficiency introduced by optical to electronic conversion. Solutions already present are based on mechanical delay lines and variable delay lines but these are very slow.

Slow light is the propagation of an optical pulse with a very low group velocity. It occurs when pulse is slowed down by the interaction with the medium in which propagation takes place. When light is input into periodic structures, reflections cause forwards and backwards travelling components of light wave to interfere. This gives a standing wave with group

velocity  $v_g=0$  at the band edge created by the periodicity [7]. Just away from the band edge, there is a region of slow light ( $v_g \ll c$ ), where the envelope of the interfering backwards and forwards travelling components moves forward only very slowly.

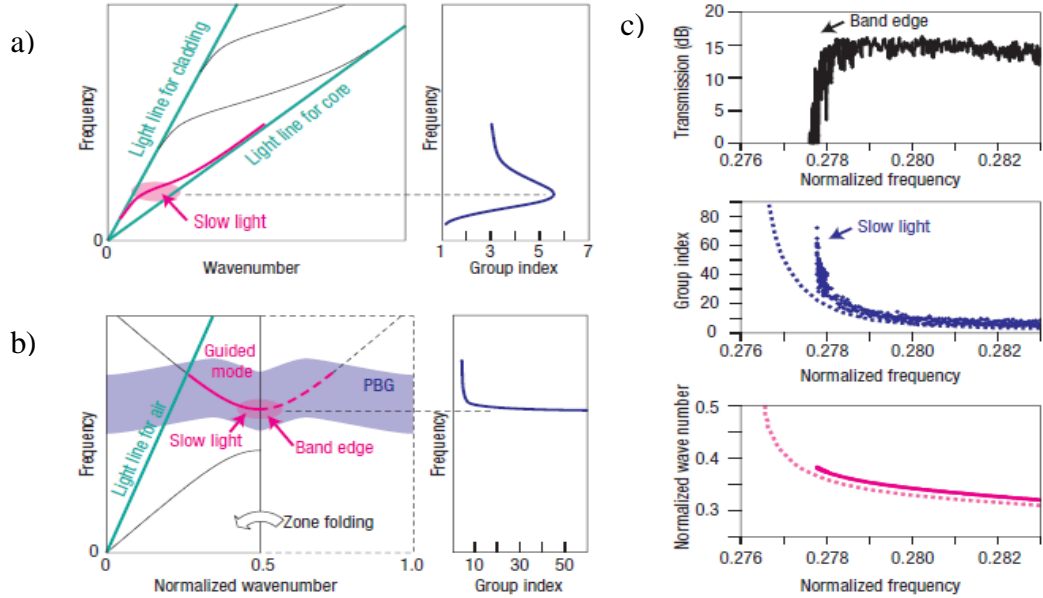


Figure 1.7: a), b) Band diagram & group-index spectrum of a silicon photonic crystal waveguide. c) Transmission spectra, group-index spectra & band diagram w.r.t. normalized frequency of a silicon photonic crystal waveguide [8].

The key feature of slow light technique is to introduce a large change in the refractive index of the medium as light propagates through that material. The change in the refractive index results in propagation of different components of an optical wave to move at different speeds and hence affects the group velocity of pulse envelope. Therefore, with dispersion of material being strong, the group velocity of light propagating in a material can be reduced to a velocity considerably less than the speed of light in vacuum. In this way, the speed of information transmission can be easily manipulated according to requirement [6]. Slow light with low group velocity in photonic crystal waveguide has gained significant amount of attention due to the fact that it can find applications in buffering and time-domain processing of optical data. It also can be used for spatial compression of optical energy and enhancement of linear and nonlinear optical effects. Slow light has been experimentally reported in various mediums, but it needs to be achieved over wide bandwidth so that can be useful in practical applications. Photonic crystal devices are outstanding choice for generating slow light, as they are well suited for on-chip integration and room temperature operation. They also

exhibit wider bandwidth and low dispersion propagation [8]. Photonic crystal line-defect waveguides are usually implemented on Silicon-on-Insulator platform due to the fact that the index contrast of silicon to air is high which results in a large photonic band gap. Furthermore, it is well-suited with conventional technology and integration of electronic and optical components on a chip is possible.

## 1.4 Optical Delay Lines

Slow light can be used in optical delay scanning and optical signal processing. Photonic crystal waveguides formed on silicon-on-insulator substrate are promising for such applications as they generate wide-band, tunable on-chip slow light at room temperature [10]. When the real and imaginary parts of refractive index change with the frequency, it causes change in the group velocity and subsequently the time delay varies. After the generation of dispersion-free slow light over a wide wavelength range, an important consideration is its wide-range tunability [11]. Variable group velocity and group delay were experimentally demonstrated for the first time for slow light by changing the index of a photonic crystal waveguide. The reported bandwidth and tuning range were small. Tunability has also been experimentally reported with the use of dispersion-compensated slow light. A large shift in optical pulses was reported by changing the material index and by engineering the device structure.

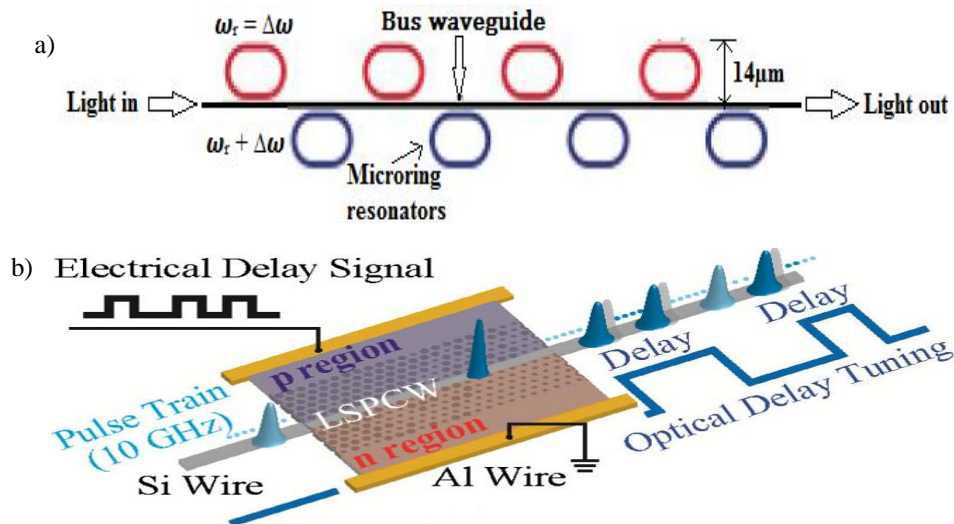


Figure 1.8: (a) Tunable delay line structure using microring resonators with central frequency  $\omega_r$ . For tuning the delay, refractive index of red rings is increased which red shifts the resonances of the rings, whereas refractive

index of blue rings is decreased which blue shifts the resonances of the rings. (b) Electrical delay tuning of slow light pulses in pin-diode-incorporated photonic crystal waveguide [13,14].

Slow light provides time delay for optical signal and is a key component for processing, storing and buffering of optical signals directly in optical format, desired in future all-optical communications and information processing systems. Dynamic tuning of slow light, i.e., tuning the light while it is present in the device, is advantageous as it provides functions, such as frequency conversion and complete stopping of light [12]. Delaying an optical signal is useful for radio-frequency photonics, and enhanced nonlinearities. Several recent research efforts have focused on replacing relatively bulky fiber-optic delay-line systems with compact integrated devices. A low  $v_g$  near the photonic band edge is not only effective for a delay line but for the enhancement of optical amplification and electro-optic effects. Reduction in  $v_g$  helps in reducing the size of devices for controlling light. Tunable optical true-time delay lines are essential components in optical beam-forming control of phased-array antennas, optical coherence tomography and optical communication networks.

Group index ( $n_g$ ) is tuned by changing material index. The easiest way of tuning is to utilize shift in the band-edge associated with change in refractive index ( $\Delta n$ ). With small  $\Delta n$ , guided mode of the photonic crystal waveguide shifts maintaining its shape. The group index changes sharply at frequencies greater than band edge. Heating and carrier plasma effect are commonly used methods to change the refractive index of the photonic crystal slab. Heating allows a large  $\Delta n$  (change in refractive index) up to 1%, and  $n_g$  was tuned in range of 20–60 using heater integrated with photonic crystal waveguide [13]. Based on the slow light technique, various methods have been developed to realize a tunable delay line. For achieving slow light dispersion is tailored. The change in index affects the data signal, and therefore, produces controllable delays. The group velocity of light is the inverse of first-order dispersion, i.e.,  $(dk/d\omega)^{-1}$  [12]

$$v_g = \frac{c}{n_g} = \frac{d\omega}{dk} \quad (1.1)$$

where  $k$  and  $\omega$  are the wave number and angular frequency. The group index is given by [12]

$$n_g = \frac{c}{v_g} = c \left( \frac{dk}{d\omega} \right) = \frac{d(n\omega)}{d\omega} = n + \omega \frac{dn}{d\omega} \quad (1.2)$$

which is regarded as slow-down factor from the speed of light. For an optical pulse having smaller bandwidth than the dispersion region, group index is directly proportional to the delay occurred during propagation [5]. If a slow-light pulse propagates through a material of length  $L$ , the delay experienced by a pulse is called group delay. If length of delay line based photonic crystal waveguide is  $L$ , then group delay is given by [12]

$$\Delta t = \frac{L}{v_g} = \frac{(n_g \times L)}{c} \quad (1.3)$$

where  $v_g$  and  $n_g$  are the group velocity and group index respectively. The time group delay  $\Delta t$  of a photonic crystal waveguide can be increased by increasing its device length  $L$  or by reducing its group velocity. Therefore, in order to increase the group delay in the device and to decrease its physical length, value of group velocity should be minimized; hence value of group index should be maximized. Tunable delay lines have been experimentally reported by changing waveguide propagation path. But this method is bulky and losses increase with increasing number of stages. Also, the delay resolution, which is determined from the shortest path, is limited to sub-nanoseconds. A tunable optical delay line should include certain essential features like large bandwidth, continuous tunability, large tuning range and fast reconfiguration speed. Such delays provide flexible time-division data grooming in the optical domain. The next section elaborates application areas in which a tunable delay line has promising potential for usage.

## 1.5 Applications of Tunable Delay Lines

In order to enhance the throughput and efficiency of reconfigurable optical networks, there is need of a wideband and tunable optical delay line [14]. Therefore optical delays, which are tunable over a wide range, are an essential building block for all optical networks for performing various functions like optical time multiplexing, synchronization, buffering and equalization. Amongst the emerging technologies for obtaining a wideband tunable optical delay line, slow light has emerged as the most promising enabler. A delay line is applicable for the purpose of synchronization for multiplexing and switching, equalization and dispersion compensation, and time-slot interchanging in dynamic networks. Slow-light-based optical delay lines can potentially be directly used for various applications in signal processing areas discussed below.

### **1.5.1 Optical synchronization and multiplexing**

For almost all types of processing, it is extremely essential to synchronize various misaligned input data bit streams to a device. Optical time-division multiplexing (OTDM) is a type of application which needs accurate allocation of every input signal into a specific time slot [11]. This ability is also required in optical packet switched networks, where for the synchronization to take place; various tasks are performed such as buffering header recognition, time switching, etc. Based on this technique various advanced modules which use packet/bit-level synchronizers can be formed. Some examples are time slot interchangers, serial-to-parallel converters, i.e., Time Division Multiplexing (TDM) to Wavelength Division Multiplexing (WDM) and parallel-to-serial (WDM to TDM) converters.

### **1.5.2 Optical equalization**

Equalizers are highly useful for mitigating the signal degradations caused due to fiber dispersion and intersymbol interference. In most of the cases, structures which utilize tapped optical delay lines are usually utilized for the designing of an optical equalizer. Tunable delay lines based on the slow-light technique are promising for application in this area as the delays generated are adjustable flexibly and accurately. This property enables wide-band tunable operation. Hence forth, it can support variable bit-rate data streams at the input. A DPSK demodulator (Differential Phase Shift Keying) based on optically tunable delay-line is also in the category of equalizer which has filter-like operation [12].

### **1.5.3 Optical correlation**

Optical correlation is an essential requirement in future all optical networks for the purpose of thresholding and pattern matching. The tunability of slow light can be improved by locally heating the photonic crystal coupled waveguide. A tunable fractional delay of 36 was obtained for picosecond pulses, which is the highest record for on-chip slow light. Considering this as a tunable resolution, it was applied to the delay scanning in the optical correlator. The sub-picosecond pulse with a scan frequency up to 2 kHz, which is at least 100 times faster than mechanical scanners in conventional correlators, was successfully observed. In addition to the delay, heaters can be incorporated to tune the target wavelength in the range of several 10 nm. Such a compact and flexible tunable delay will allow one-chip correlation systems.

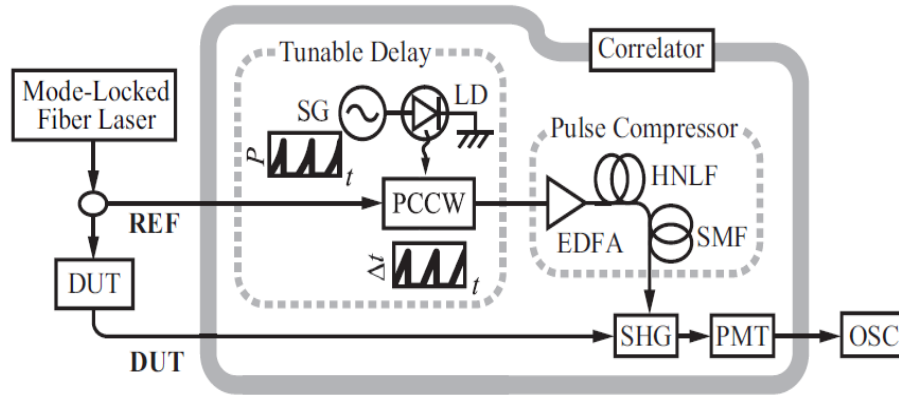


Figure 1.9: Cross-correlator using locally heated photonic crystal coupled waveguide and pulse compressor [13].

Optical correlators are widely used to observe femtosecond to picosecond-wide optical pulses. They usually utilize a mechanical delay scanner with scan frequency  $f$  up to 10 Hz. A much faster scanner is required for high-volume multi-dimensional data acquisition in optical coherent tomography and terahertz time-domain spectroscopy [13]. The delay and stack function which is fundamental to an optical correlator imposes the stringent requisite of a high tuning resolution and a fast tuning speed. A delay line based on slow light has potential to match up these requirements. Hence it has potential for utilization in optical correlators.

#### 1.5.4 Optical logic gates

The future all-optical networks, which have the hard line target of achieving processing rates greater than 100 Gbit/s, require executing of all the logic operations solely in the optical domain. It is essential requirement for the bit-rate transparency [14]. The tunable delay lines based on slow light have high potential to find promising usage in applications like complicated checksum processing based on loop-adder technique, differential phase encoders and XOR-type parity checks.

#### 1.5.5 Enhanced nonlinear interaction

A small change in the refractive index gives rise to increase in the induced phase shift in the device. Hence forth, with reduction in the group velocity of light, nonlinearities in the device can be enhanced. Various methods can be employed for changing the refractive index. By using the increased nonlinear phase shift associated with change in refractive index, a large number of applications can be realized like wavelength multicasting, optical switching, 2R/3R regeneration, wavelength conversion, etc. [14].

To obtain a large delay of the data signal with very small amount of system power, signal degrading effects associated with slow light have to be compensated. The data fidelity should be maintained and this issue needs to be dealt with before any signal processing modules are designed practically.

## **1.6 Purpose and Outline of Thesis**

The purpose of our research is to design and analyze graphene based photonic crystal waveguide for optical delay tuning applications. The advantage of graphene's electrical tuning is taken into account for tuning the group delay in a line-defect photonic crystal waveguide. The introduction of few-layer-graphene (FLG) into photonic crystal waveguide can slow down the light. FLG being a semi-metal forms surface plasmon polariton (SPP) [15] with the guided mode in PCW which increases group index of the guided mode resulting in slowing down the light. Further, application of electric field on graphene can tune its Fermi-level which causes a change in group delay. Presence of graphene not only provides the way to electrically tune the delay with low-power but it also enhances the group delay. The design and analysis are performed with plane wave expansion method (PWE) [16, 17] using software MIT Photonic Bands (MPB) [18]. The layout of the thesis is as follows:

Chapter 2 discusses the fundamental optical properties of graphene and discusses some examples of graphene devices which are the background of the present work.

Chapter 3 presents a brief survey and review of the published research work on graphene and photonic crystal waveguides.

Chapter 4 discusses the methodology of photonic crystal modeling and proposed design of graphene based photonic crystal waveguide. In first design, graphene layer is placed on top of waveguide (line-defect). In second design, graphene is placed on the holes (clad). Calculation of group delay at communication wavelength is done for different electric field values. Delay tuning is reported by varying the applied electric voltage on graphene.

Chapter 5 discusses the concluding remarks and elaborates on future research directions for the work.

# CHAPTER 2

## Graphene based Optoelectronic Devices

### 2.1 Introduction

Graphene is a single layer of carbon atoms forming a hexagonal lattice. It can be also thought of as a single layer of graphite, which consists of a stack of atomic layers of hexagonal lattices. Graphene offers great possibilities for scientific and technological developments. It is one of many allotrope modifications of carbon among other dimensionally reduced structures such as fullerenes, carbon nano tubes and nano fibers, etc. It consists of  $sp^2$  hybridized carbon atoms arranged into a two-dimensional (2D) honeycomb lattice. It the basic building block for carbon materials of other dimensions. Graphene can be wrapped into 0D fullerenes, rolled into 1D nano tubes, or stacked into 3D graphite [19].

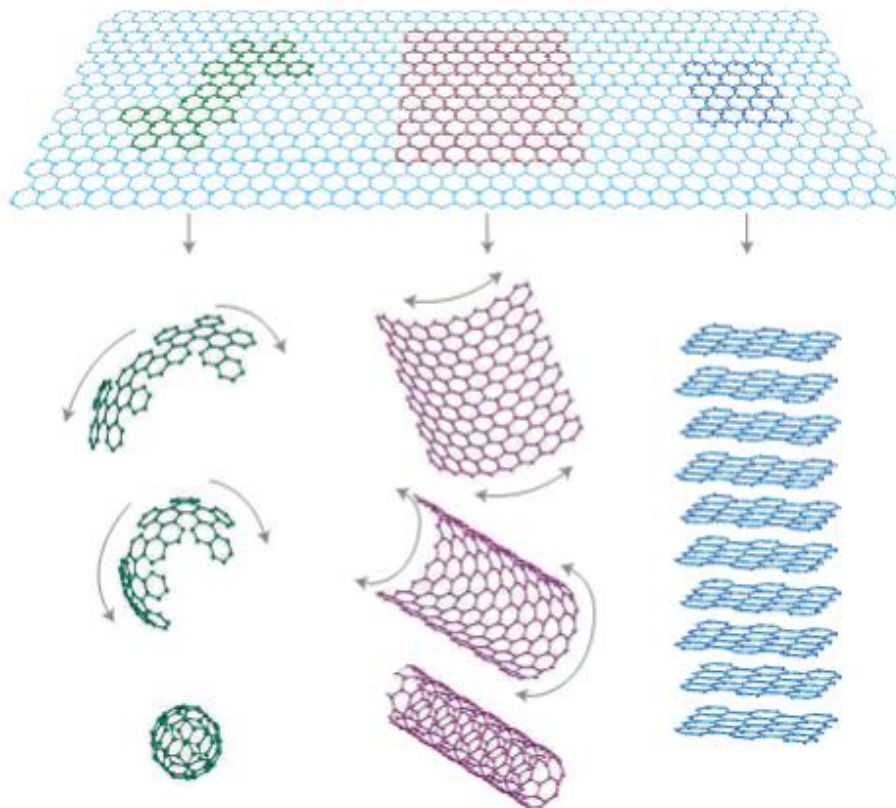


Figure 2.1: Graphene as a two dimensional building material for carbon materials of other dimensions. It can be wrapped into 0D fullerenes, rolled into 1D nano tubes or stacked into 3D graphite [19].

Theoretically graphene (or monolayer graphite) has been studied for the last sixty years. The theoretical studies of graphene were undertaken first by Wallace. The outstanding properties of graphene come from its unique crystal structure. It can be considered as two triangular sub lattices with two carbon atoms per unit cell. The band structure of graphene can be described by a pair of Dirac cones. At absolute zero temperature, the Fermi energy is at the charge neutrality point (Dirac point) where the lower energy cone is completely filled while the upper one is empty. Because of low density of states in graphene, its chemical potential can be modulated by an external gate voltage to populate electrons to the upper cone or deplete electrons from the lower cone. Thus, the tunability of chemical potential is a key to electrically regulating the optical transition of graphene-based devices.

The absence of band gap makes graphene a semi-metal, distinguishing itself from other semiconductor material. It exhibits constant conductivity at optical frequencies and acts as a nonlinear optical medium. These unique properties may be utilized in future electronic and optoelectronic devices. The unique optical properties of graphene have been applied to create gas sensors, plasmonic resonators in terahertz, and electro-absorption optical modulators at 1550 nm wavelength. The excellent electrical properties of graphene, such as high carrier mobility and electrical conductivity, have been well studied and applied to build high-frequency field effect transistors [21].

Graphene demonstrates various characteristics similar to Dirac fermions like fractional quantum Hall effects, Haas oscillations with  $\pi$  phase shift and minimum conductivity of  $\sim 4e^2/h$  even when carrier concentration approaches zero. Mobilities ( $\mu$ ) of up to  $106 \text{ cm}^2\text{V}^{-1}\text{s}^{-1}$  are observed in suspended samples [22]. Due to all these properties, graphene is a highly promising material for usage in nanoelectronics, chiefly in high-frequency applications. The Dirac electrons exhibit linear dispersion which makes usage in broadband applications possible.

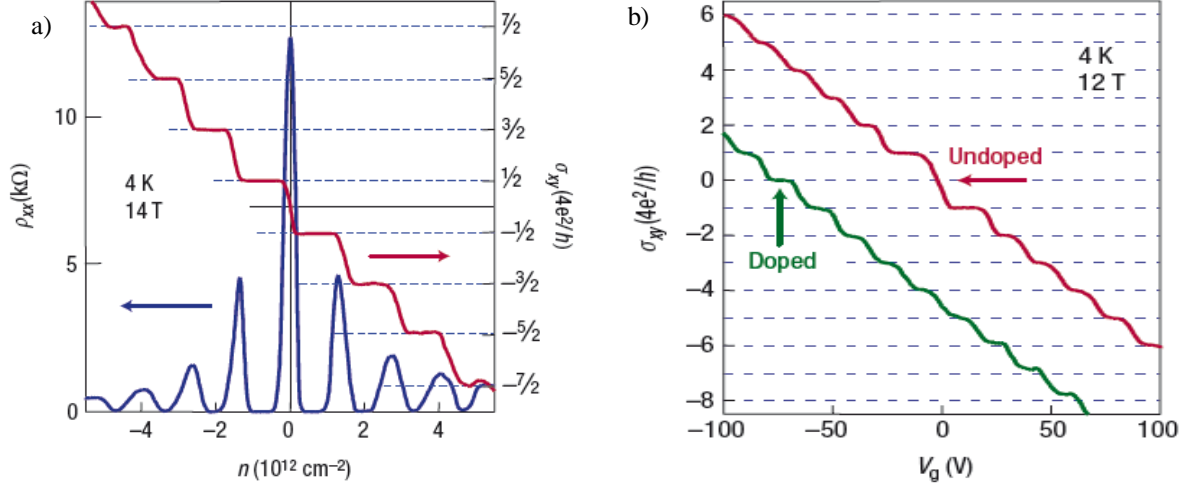


Figure 2.2: Chiral quantum Hall effect (QHE). a) The characteristic of massless Dirac fermions is a visible QHE plateau. b) Anomalous QHE for Dirac fermions is more subtle in bilayer graphene (red curve). The region where plateau is missing is shown by red arrow. Green curve indicates the zero- $N$  plateau can be obtained again by chemical doping of graphene, which results in the shifting of the neutrality point to high voltage so that an asymmetry gap ( $\approx 0.1\text{eV}$ ) is opened by the electric field effect [19].

A tunable band gap which was gate controlled up to 250 meV has been experimentally reported in bilayer graphene [23]. Due to the effect of intra-band absorption, the magnitude of graphene dielectric constant can be dynamically tuned in a large range by electrical gating. The expression for the conductivity of graphene contains two significant contributions: interband electron transitions and intraband absorption. The chemical potential equivalent to the Fermi level describes the maximum energy occupancy level of electrons in the material. For pure undoped graphene, there are only electrons in the valence band and chemical potential is zero. The chemical potential can be adjusted through chemical doping or from applying a voltage between the graphene and an underlying substrate (electrostatic doping). This allows for the conductivity and consequently, the optical absorption, to be highly tunable. Using Kramer–Kronig relation, optical conductivity  $\sigma$  of graphene can be written as [24]

$$\sigma_1(\omega) = f(\omega) + \frac{q^2\Gamma}{2\pi\hbar^2} \frac{1/\tau}{\omega^2 + (\frac{1}{\tau})^2} \log\left(2 \cosh \frac{2E_F}{\Gamma}\right) \quad (2.1)$$

$$\sigma_2(\omega) = -\frac{2\omega}{\pi} \int_0^\infty \frac{f(\omega') - f(\omega)}{\omega'^2 - \omega^2} + \frac{q^2\Gamma}{2\pi\hbar^2} \frac{\omega}{\omega^2 + (\frac{1}{\tau})^2} \log\left(2 \cosh \frac{2E_F}{\Gamma}\right) \quad (2.2)$$

with 
$$f(\omega) = \frac{q^2}{8\hbar} \left[ \tanh\left(\frac{\hbar\omega + 2|E_F|}{\Gamma}\right) + \tanh\left(\frac{\hbar\omega - 2|E_F|}{\Gamma}\right) \right] \quad (2.3)$$

Here  $\sigma_1(\omega)$  and  $\sigma_2(\omega)$  are the real and imaginary parts of optical conductivity of graphene respectively,  $q$  is the electronic charge and  $\Gamma$  is the interband transition broadening. The free carrier scattering rate  $1/\tau$  is in terahertz range, and can be neglected for electromagnetic waves in the near infrared and visible frequencies.  $E_F$ ,  $\epsilon_0$ ,  $\hbar$  and  $\omega$  are the graphene Fermi energy, vacuum permittivity, reduced Planck's constant and angular frequency, respectively. The Fermi level of graphene ( $E_F$ ) and applied voltage ( $V$ ) can be related as [25]

$$E_F = \hbar v_F \sqrt{\pi \left( n_0 + \frac{C|V|}{q} \right)} \quad (2.4)$$

where  $C$  is effective capacitance per unit area,  $v_F \sim 10^6$  m/s is Fermi velocity for graphene, and  $n_0$  is intrinsic carrier concentration. Effective capacitance of ion gel gating  $C \sim 20$  mF/m<sup>2</sup> and any intrinsic carrier concentrations are neglected. The complex dielectric function  $\epsilon_g(\omega)$  of graphene can be obtained from the corresponding optical conductivity  $\sigma(\omega) = \sigma_1(\omega) + i\sigma_2(\omega)$  using [23]

$$\epsilon_g(\omega) = 1 + i\sigma(\omega)/\epsilon_0 \omega dg \quad (2.5)$$

where  $\epsilon_0$  is the permittivity of free space,  $\sigma(\omega)$  is frequency-dependent conductivity of material,  $dg$  is effective thickness of layer and  $\omega$  is angular frequency of light. The imaginary part of  $\epsilon_g(\omega)$  (responsible for the light absorption) decreases monotonically with increasing voltage, especially when  $2|E_F|$  is larger than resonance energy  $E_r$  and blocks relevant interband transitions. On the other hand, real part of  $\epsilon_g(\omega)$  is a non-monotonic function of the applied voltage. This is because  $\sigma_2(\omega)$  has significant contribution from both intraband and interband transitions. Contribution from intraband transition increases monotonically with increasing  $|E_F|$ . The contribution from the interband transitions exhibits minima at  $2|E_F| = E_r$ . The real ( $\epsilon_g'$ ) and imaginary ( $\epsilon_g''$ ) part of graphene dielectric constant vary upon electrical gating. The imaginary part  $\epsilon_g''$  is affected by constant absorption of  $(\pi e)^2/c$  from the interband transitions and Drude absorption from free carriers. The real part  $\epsilon_g'$  can be obtained from  $\epsilon_g''$  using the Kramer–Kronig relation. Specifically,  $\epsilon_g'$  and  $\epsilon_g''$  can be given by [25]

$$\epsilon'_{\mathbf{g}}(E_{\mathbf{F}}) = 1 + \frac{e^2}{8\pi E \epsilon_0 d} \ln \frac{(E + 2|E_{\mathbf{F}}|)^2 + \Gamma^2}{(E - 2|E_{\mathbf{F}}|)^2 + \Gamma^2} - \frac{e^2}{\pi \epsilon_0 d} \frac{|E_{\mathbf{F}}|}{E^2 + (\frac{1}{\tau})^2} \quad (2.6)$$

$$\begin{aligned} \epsilon''_{\mathbf{g}}(E_{\mathbf{F}}) = & \frac{e^2}{4E \epsilon_0 d} \left[ 1 + \frac{1}{\pi} \left\{ \tan^{-1} \frac{E - 2|E_{\mathbf{F}}|}{\Gamma} - \tan^{-1} \frac{E + 2|E_{\mathbf{F}}|}{\Gamma} \right\} \right] \\ & + \frac{e^2}{\pi \tau E \epsilon_0 d} \frac{|E_{\mathbf{F}}|}{E^2 + (\frac{1}{\tau})^2} \end{aligned} \quad (2.7)$$

where  $E_{\mathbf{F}}$ ,  $\epsilon_0$  and  $d$  are Fermi energy, vacuum permittivity and thickness of graphene. Thickness of graphene is taken as  $\sim 1$ nm for the calculations. It is equivalent to few layer graphene which acts like a semi-metal. The free carrier scattering rate  $1/\tau$  has very small effect on the dielectric constant. Therefore, it is taken as zero. The interband transition broadening  $\Gamma$  is predicted to be 110 meV. Equation (2.7) shows that the imaginary part of dielectric constant shows a step-like decrease when  $2|E_{\mathbf{F}}|$  is greater than the resonance energy  $E_{\mathbf{R}}$ . The real part has contribution from both the intraband and interband transitions. The contribution of intraband transition decreases monotonically with carrier doping. The interband transition contribution is maximum at the point where  $2|E_{\mathbf{F}}| = E_{\mathbf{R}}$ . This is due to the fact that the optical transitions below resonance energy contribute negative susceptibility and those above the resonance energy contribute positive susceptibility.

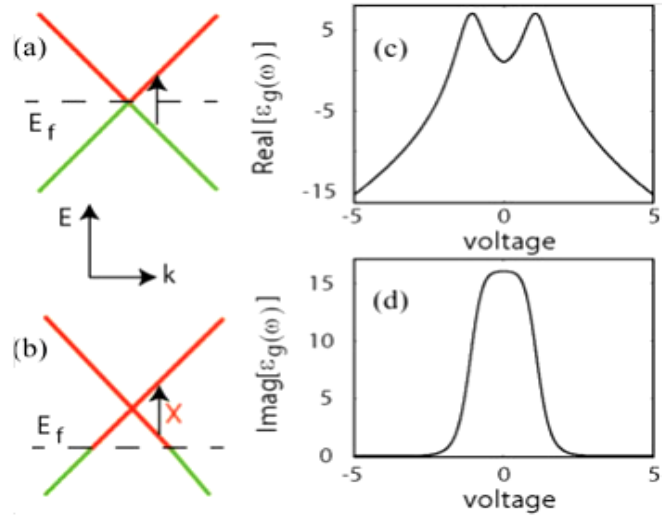


Figure 2.3: (a) Band diagram of graphene showing linear dispersion of carriers near Dirac point, where conduction and valence band meet. The Fermi energy is at Dirac point, and graphene can absorb a light with frequency corresponding to arrow. (b) If Fermi energy is shifted under application of an electric field, then light

cannot get absorbed in graphene anymore. (c), (d): Real and imaginary part of the refractive index of graphene as a function of the applied gate voltage [26].

## 2.2 Applications of graphene in optoelectronic devices

Due to its extremely high mobility, graphene is considered a promising material for ultra-high speed electronics, digital logic and interconnects. Apart from exhibiting a high mobility, graphene possesses various other unique optical, electrical, thermal and mechanical properties that constantly inspire innovations. Graphene is an excellent channel material for devices in radio-frequency applications. First of all, its ultra-high mobility, which leads to micrometer-scale ballistic transport, together with very large saturation velocity, brings graphene enormous potential for high-frequency devices. In addition, the outstanding thermal conductivity and micrometer-scale ballistic transport inspire great hope for using graphene in low-noise amplifiers. In this section, the progress in the research for the applications of graphene in the optoelectronic devices is reviewed.

An electro-optic modulator based on the concept of electrostatic gating was demonstrated by Liu et al. in 2011 [27]. The device consists of graphene placed on top of a doped silicon waveguide designed to guide light at a wavelength of  $1.53 \mu\text{m}$ . The waveguide is physically separated from the graphene using a  $7\text{nm}$  thick  $\text{Al}_2\text{O}_3$  layer. The graphene layer is electrically connected to an Au-Pt electrode, whereas silicon waveguide is in contact with other electrode. Using an applied voltage across two contact pads, chemical potential (Fermi level) of graphene is tuned such that the absorptive properties of graphene are also tuned.

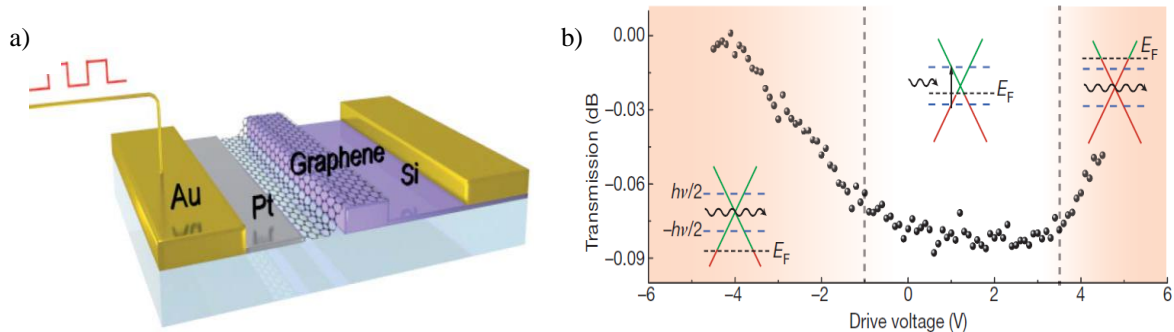


Figure 2.4: (a) Schematic of electro-optic modulator device from Liu et al. (b) Transmission of optical signal vs. drive voltage applied to the gold contact pads. There are three distinct regions of operation, which correspond to the shifting of the Fermi level [27].

For drive voltages lower than -1V, Fermi level is below the interband transition energy. This prevents any electrons from being available for interband transitions. For drive voltages near 0V, Fermi level is near zero and graphene is highly absorptive since electrons are now available for interband transitions. For drive voltages greater than 3.8V, Fermi level is large enough that electrons occupy all of the possible transition states that are in resonance with any photons, so photons are not absorbed. The minimum transmission is offset from zero-bias because the silicon waveguide is doped with boron (a p-type dopant), which shifts the Fermi level negatively. Modulation depth, which is the ratio between maximum and minimum transmission in the device, was found to be 0.1dB/ $\mu\text{m}$ .

Graphene can be used to transport surface plasmon polaritons (SPPs) along it. SPPs are created when light couples to free electrons on surface of a metal. Light can be confined into a much smaller modal area and the effective wavelength of light is much smaller than the free-space wavelength. Plasmonics can be used to make photonic devices that circumvent the diffraction limit of light. Plasmonic waveguides, which allow for the sub-wavelength propagation of light, can also be realized with graphene as reported by Kim et al. [15]. Graphene was transferred on a cladding layer ( $n=1.37$ ) of thickness  $20\mu\text{m}$ . It was patterned into strips that were 5.7mm long. Another cladding layer of  $20\mu\text{m}$  was then placed on top. Light of wavelength  $1.31\mu\text{m}$  was coupled onto the graphene strip using a polarization-maintaining fiber. Coupling loss was measured to be 1dB per facet for TM-polarization and propagation loss for TM-polarization was 2.1dB/mm. The corresponding propagation length is approximately 2.1 mm, which is considered to be long compared to conventional metal-dielectric material systems. Surface plasmons propagating along top and bottom surfaces of graphene form a well-confined guided mode.

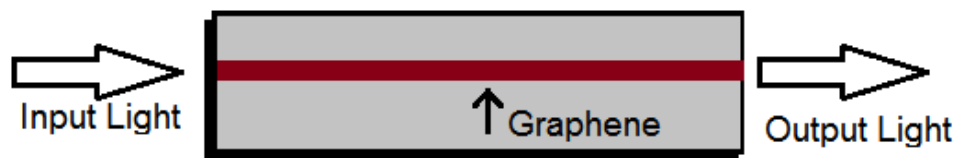


Figure 2.5: Schematic of graphene waveguides by Kim et al. Graphene strips of length 5.7 mm are patterned between a  $20\mu\text{m}$ -thick dielectric on both sides [15].

The output power was measured as a function of the polarization of incoming light and it was found that when TE-polarized light is used, the insertion loss increases by 19dB compared to TM-polarized light. This demonstrates that the performance of graphene plasmonic

waveguide has strong polarization dependency. To demonstrate practicality of plasmonic waveguide, light pulses encoded with pseudorandom data were transmitted along the graphene strip at a rate of 2.5 Gbps. Bit-error-rate was measured to be  $10^{-10}$  which demonstrates that virtually all of the data was readable at the output.

Zhou et al [28] demonstrated enhanced four-wave mixing in a graphene based photonic crystal waveguide. Four-wave mixing conversion efficiency of -23 dB was achieved with this design. Their measurements matched fit with nonlinear coupled-mode theory simulations. This idea proposes an effective way for optical signal processing on chip-scale integrated optics. In large scale integrated circuits and systems, interconnects have become more and more critical for chip performance. When used as interconnects, graphene also shows a great potential. The conductivity of graphene nano-ribbons is expected to surpass copper wires when the width of the optical interconnects is less than 8 nm. It is also predicted that high-quality graphene nano-ribbon offers a much smaller signal delay than that offered by copper. The graphene nano-ribbons possess breakdown current density of about  $108 \text{ A/cm}^2$ , which is approximately ten times greater than the current density of copper. Graphene has high Kerr nonlinearity as large as  $n_2=10^{-7} \text{ cm}^2/\text{W}$ . By increasing of intensity of pump light, refractive index of graphene increases by a large amount due to Kerr nonlinearity, shifting the Fano resonance frequency in the photonic crystal slab [29]. This property finds application in phase shifters and phase modulators, optical phase logic devices for optical computations and optical phase shift-keying in communication systems.

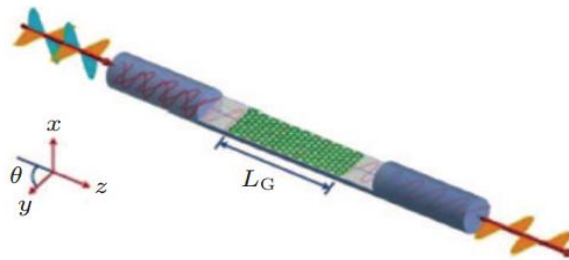


Figure 2.6: Schematic model of fiber-to-graphene coupler based on a side-polished optical fiber; here  $L_G$  is the propagation distance (length of covered graphene film).

Polarizers, which convert a beam of light with undefined or mixed polarization into a beam with well defined polarization, are crucial passive components in optical systems. Current polarization controlling devices can be classified into sheet polarizers using anisotropic absorption media, prism polarizers by refraction, and Brewster-angle polarizers by reflection,

which are all bulky and difficult to integrate with photonic circuits. The in-line fiber polarizer is a promising alternative. In the conventional two-dimensional electron systems, only the transverse-magnetic mode can propagate. The spectra of electromagnetic modes are electron (hole) mass sensitive. Therefore, with massless Dirac fermions, graphene paints a radically new picture. By shifting the Fermi level, graphene can selectively support either the transverse-magnetic (TM) or transverse-electric (TE) electromagnetic modes, which provides the basis for graphene polarizers that transform unpolarized incident light into polarized light. Bao et al. fabricated an optical fiber polarizer with graphene as an in-line conductive layer. A TE mode extinction ratio up to  $\sim 27$  dB has been demonstrated, covering very broad communication bands. Millimeter-scale graphene with high continuity and uniformity is needed in this kind of device. A schematic diagram of the device is shown in Figure 2.6.

### **2.3 Tunable optoelectronic devices based on graphene**

In order to enhance the interaction of photons with graphene various nanophotonic device designs have been proposed. Waveguides and cavities are types of such nanophotonic devices which make strong enhancement in the light interaction with graphene possible. Due to small atomic thickness graphene is highly transparent but it exhibits strong interaction with photons. This offers numerous advantages over materials which are used in existing photonic devices like Indium-based compounds. Graphene has another interesting usage. It can be utilized to trap light. It can also find applications in altering the wavelength of incident light. These significant properties form the foundation of the plasmonic devices. Graphene is highly transparent over a wide range of wavelengths from the visible to the near-infrared. The optical absorption in graphene is independent of wavelength, covering all the infrared range and as well as the telecommunications bandwidth.

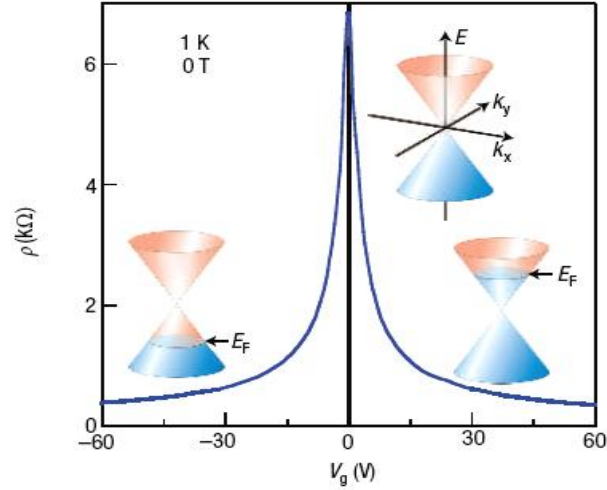


Figure 2.7: Electric field effect in single graphene layer. The insets indicate changes in the position of Fermi energy  $E_F$  with changing gate voltage  $V_g$ . Positive (negative)  $V_g$  induces electrons (holes). The swift reduction in the resistivity  $\rho$  on the addition of the charges signifies high mobility [19].

Majumdar et al. [31] reported a significant change in the resonance of a photonic crystal cavity by electrically gating graphene layer on top of the cavity. Ion gel gating is used in the device for the purpose of electrical gating. An approximate  $\sim 2\text{nm}$  change in cavity resonance line width and about 400% (6dB) change in resonance reflectivity were experimentally reported. This demonstrated that a graphene based photonic crystal device has potential to be used as a low power absorptive/refractive modulator which has high modulation speed and very small physical device size.

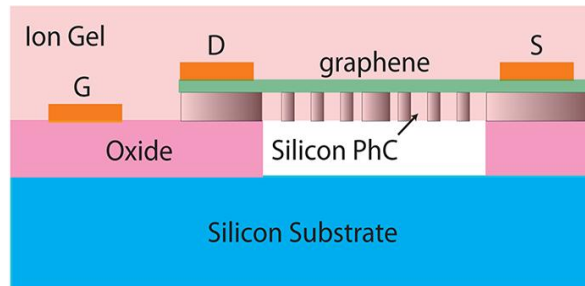


Figure 2.8: Cross sectional view of the photonic crystal cavity device using graphene. The cavity is fabricated on silicon-on-insulator platform. The electrical gating is performed using drain, source, and gate. These contacts are covered by an ion-gel [31].

Surface plasmons have been experimentally shown to concentrate light inside sub-wavelength volume. Controlling the resonance of plasmons at optical frequencies is very difficult because free electrons have extremely feeble response at optical frequencies. A

unique hybrid graphene-gold nanorod system was proposed and effective control of plasmon resonances in the near infrared region was experimentally demonstrated [32]. Graphene possesses strong optical transitions which are gate-tunable. By efficiently utilizing these, the quality factor and the resonance frequency of the proposed hybrid system can be modulated. The observed plasmon-graphene coupling in the device is extraordinarily strong. Therefore, this type of proposed hybrid structure has the potential for remarkable and efficient control of plasmon resonances electrically at optical frequencies. This could help in realizing devices that enable novel plasmonic sensing.

Using graphene on planar photonic crystal nanocavities helps to selectively enhance the coupling of light with graphene. A significant enhancement in the absorption of the cavity based device was observed. Various other phenomena like hot photoluminescence and Raman scattering of a graphene layer were elaborately discussed in the proposed design [33]. The usage of graphene in photonic crystal nano-cavity enables enhancement in the light-matter interaction. A transmission attenuation of about 6.2dB was reported over  $70\mu\text{m}$  waveguide length.

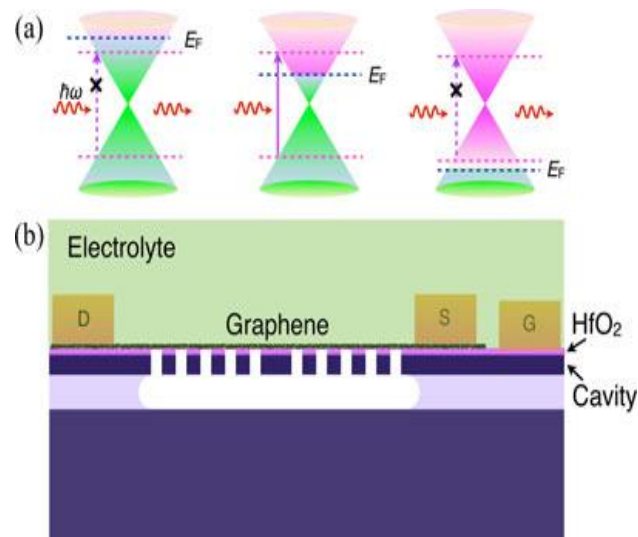


Figure 2.9: (a) Band structure of graphene at various doping levels. As depicted in the images on left and right, transparency of graphene increases when interband transitions are Pauli blocked. (b) Cross sectional view of the graphene based Photonic crystal nano-cavity which is electrically controlled. A thin  $\text{HfO}_2$  layer is used for the electrical isolation of silicon and graphene. The reflection in the cavity is modulated through the fermi level tuning. In graphene via doping fermi level is tuned [33].

A unique type of photonic crystal device design using graphene was proposed by L. Berman. The photonic crystal is fabricated in a new way by implanting a group of alternating graphene discs and dielectric discs stacks periodically into a background dielectric medium. Theoretically, it is predicted that for far-infrared area of electromagnetic spectrum, graphene-based photonic crystals can find applications as waveguides and frequency filters. Doped graphene is used which helps in reducing absorption of low-frequency radiation. Therefore, the skin effect and damping effect in the photonic crystal were reported to be suppressed. The device structure consists of a two dimensional photonic crystal. The stacks of graphene discs are placed periodically. These are implanted into the dielectric film. A stack is formed by placing graphene discs on top of each other. These are separated by dielectric placed between them. The dielectric photonic crystals find usage only in the optical region of spectrum. So the idea behind proposing such type of photonic crystal is that these types of devices with the metallic constituent elements can potentially find usage in the far-infrared region of spectrum.

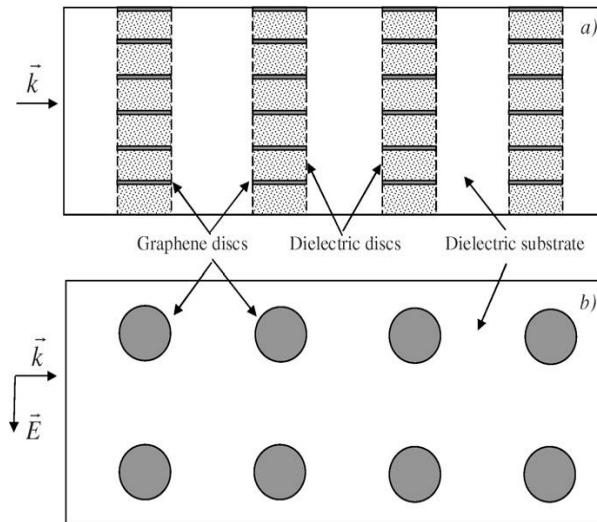


Figure 2.10: a) Cross-sectional view and b) Top view and of the graphene-based photonic crystal [34].

The graphene based photonic crystal device design reported above can be useful at a wide range of temperatures. Various optimizations can be made to the structure to suit the requirement of an application. In order to vary the band structure of this design, thickness of dielectric layers can be changed which are between the graphene discs. The doping of graphene can also be varied according to the requirement.

## 2.4 Use of Graphene for Delay Tuning

Slow light with significantly reduced group velocity has been intensively studied for the tuning of optical delays. Slow light provides effective and variable interaction with the device material resulting in a tunable delay in a compact device. Tunable delays are essential components in the optical communication networks. Different approaches like stimulated brillouin scattering, stimulated raman scattering, microring resonators and wavelength conversion have been demonstrated for tunable delays. However, these approaches have limitations such as large device size, high precision fabrication, high power requirement, etc. Therefore, silicon photonics has been considered for generating tunable delays. Photonic crystal waveguides fabricated on silicon on insulator are promising for the delay tuning applications as these generate on-chip wide-band and tunable slow light [12].

Photonic crystal line-defect waveguides have also been proposed and implemented for tuning the group delay. In these structures, thermo-optic effect [34] and electro-optic effect [35] are the methods employed for implementing delay tuning. The thermal change of optical refractive index in Si is large. However, thermo-optic effect is slow and there exist issues regarding the mechanism used for heating the device. It is challenging to control the temperature rise only to the locality of such tiny structures. Silicon has low electro optic coefficient and this poses a challenge when it is used as active photonics material. A change in refractive index of about  $\Delta n \sim 10^{-5}$  for Franz keldysh effect and  $\Delta n \sim 10^{-8}$  for Kerr effect for an applied electric field of  $10^5$  V/Cm is observed [36]. Therefore, in order to obtain a useful change in refractive index of Si, high values of electric voltage are required which is not suitable for low power delay tuning applications. Evidently, simultaneous achievement of a low-loss, fast, compact, wavelength-independent, high-resolution and electronically-tunable optical delay line is lacking.

Electrically tunable delay line with wide tuning range is currently in demand. Graphene has attracted extensive research interest in the recent years due to its unusual electronic and optical properties. Electrical control of graphene can pave the ways to tune group delay. Its properties can be efficiently controlled through applied electric voltage; therefore, a graphene based photonic crystal waveguide design has been proposed in order to control the transmission of light through the waveguide by the use of electric voltage. Due to its unique atomic arrangement, the conduction and valance bands meet at a single point known as the

Dirac point. The density of states of carriers near the Dirac point is low, so fermi energy of graphene can be tuned considerably with relatively low electric voltage. Graphene has the ability to be integrated with the existing wave-guiding materials like silicon. Therefore, in this dissertation the advantage of graphene's electrical tuning is taken into account for tuning the group delay in a line-defect photonic crystal waveguide. The introduction of few-layer-graphene (FLG) into photonic crystal waveguide can slow down the light. FLG being a semi-metal forms surface plasmon polariton [15] with the guided mode in the photonic crystal waveguide which increases group index of the guided mode resulting in slowing down the light. Further, application of electric field on graphene can tune its Fermi-level which causes a change in group delay.

# Chapter 3

## LITERATURE REVIEW

The simplest photonic crystal consists of alternating layers of materials with different dielectric constants. Lord Rayleigh was the first person to investigate the multilayer films and their optical properties. This one dimensional photonic crystal behaves as a Bragg mirror for specific frequency light. If a defect occurs in the structure, then it localizes the light modes. These concepts are commonly used in dielectric mirrors and optical filters. The traditional way to analyze this system, pioneered by Lord Rayleigh is to imagine that a plane wave propagates through the material and to consider the sum of multiple reflections and refractions that occur at each interface. Since Kostya Novoselov introduced the micromechanical cleavage method that produced graphene in relatively high quality; graphene has become a subject of intense interest in the research community. Research methodologies developed within the last decade in the field of photonic crystal waveguides and graphene are presented below.

**M. Notomi, *et al.* in 2001 [5]** discussed the photonic crystal waveguide with line defects which has waveguide and group velocity dispersion characteristics different from conventional waveguides. These characteristics can be tuned by controlling the defect width which results in control of light transmission through light path. A large value of group velocity is reported in interference transmission window which is achieved by tailoring various parameters of slab such as length and thickness of slab, thus achieving slow light that allows the guided modes to travel with velocity lower than that of light in vacuum.

**S. Noda, *et al.* in 2002 [2]** discussed the various types of waveguides in two dimensional photonic crystals and it was found that these structures could be implemented in three dimensions without any fabrication complexities. It has been reported that the linear waveguides in photonic crystal slabs having finite height are different from the waveguides which are vertically confined.

**N. Moll, *et al.* in 2003 [37]** investigated butt coupling into photonic crystal waveguides for a three-dimensional photonic crystal and a two-dimensional photonic crystal slab having

triangular lattice structure. The slab structure is fabricated on silicon-on-insulator platform. The transmission spectrum was found to be drastically different for both. In the case of photonic crystal slab, only a small range of frequencies are possible in which guided mode can possibly exist.

**C. Barrios, *et al.* in 2003 [38]** proposed and fabricated two designs on silicon-on-insulator substrate. The improvement in transmission of single line-defect planar photonic crystal waveguide is done for realization of planar photonic crystal by optimizing the structure with modification in shape and size in photonic crystal lattice to reduce the scattering losses.

**K. Novoselov, *et al.* in 2004 [19]** introduced the micromechanical cleavage method that produced graphene in high quality. Since then, graphene has become a subject of intense interest in the research community. Investigation of both the electronic and optical properties of graphene has been done. Graphene is a one-atom-thick with extraordinary optical and electrical properties that can be utilized in many potential applications.

**A. Vlasov, *et al.*, in 2005 [10]** demonstrated a huge amount of reduction in the group velocity of slow-light propagating in the photonic crystal waveguide. The photonic crystal is two dimensional and is fabricated using silicon. The slab is fabricated on SOI platform. It was also experimentally demonstrated that the group velocity can be effectively controlled in a fast manner by utilizing the thermal heating. The photonic crystal waveguide was locally heated using a micro-heater embedded in the chip.

**S. Noda, *et al.*, in 2006 [39]** elaborately discussed the two dimensional photonic crystals in combination with a one-dimensional Bragg mirror. The structure is proposed in order to control the out of plane coupling of modes. It also helps in controlling the quality factor. Quality factor can be enhanced varying the thickness of the two dimensional photonic crystal silicon layer etching. Several optical properties of such structure have been characterized well. A similar enhancement could be obtained by varying the thickness of the oxide layer separating the Bragg mirror and the two dimensional photonic crystal slab layer.

**Shanhui Fan, *et al.*, in 2006 [3]** discussed recent advancements in the theory of photonic crystals that exhibit the large optical physics effects and provide new ways to do optical information processing tasks more sophisticatedly and perfectly allow the announce of

dynamics into photonic crystals system and also would be able to create new optical signal processing functionalities far beyond the capabilities of the static systems.

**L. Frandsen, *et al.* in 2006 [7]** demonstrated varying the dispersion properties of the photonic crystal structure thereby resulting in variation in group velocity of slow light propagating in the photonic crystal waveguide. It was reported that the bandwidth could be increased and by disturbing the characteristics of the holes adjacent to the line-defect group velocity dispersion could be altered according to the requirement. These types of waveguiding devices can be used for pulse shaping and dispersion compensation.

**Fengnian Xia, *et al.* in 2006 [40]** presented on-chip optical delay line based waveguide that consisted of a large number of microring resonators which were cascaded in either coupled-resonator or all-pass filter configurations. They also analyzed trade-offs between resonantly enhanced group delay, device size, insertion loss and operational bandwidth for various delay-line designs.

**T. F. Krauss in 2007 [9]** discussed the physical principles and practical limitations of slow light propagation in photonic crystal waveguides. Slow light effects in photonic crystal waveguides are most advantageously employed to increase linear effects, such as thermo-optic and electro-optic tuning as well as gain and nonlinear effects such as Raman amplification, Kerr-based switching and possibly parametric effects such as wavelength conversion, delay lines are also possible. Broadband and slow light enhanced all-optical functions such as switches and modulators can be realized by careful device design to overcome the dispersion limitation by creating a broadband linear response, to avoid the backscattering losses encountered at the band-edge and to inject light efficiently.

**A.K. Geim, *et al.*, in 2007 [19]** reviewed the research on material graphene in the recent years. Graphene is a single layer of carbon atoms arranged in honeycomb lattice. It is basic building block of all other dimension carbon materials. Optical properties of graphene can be easily controlled by applying an electric field. It has extremely high carrier mobility, enabling high-speed operation. It can absorb light over a broad frequency range. Fermi energy of graphene can be tuned significantly with relatively low electrical energy, which in turn changes the refractive index of graphene. Thus, combining graphene with nano photonic

structures has tremendous potential for achieving electro-optical tunability of light transmission.

**Nakamura, *et al.*, in 2008 [22]** discussed the two-dimensional graphene monolayer and bilayer which exhibit fascinating electrical transport behaviors. They have strong inter-band transitions. The optical transitions in graphene layer can be considerably tailored by the use of electrical gating. Therefore band structure of graphene can be optically probed due to the electric field dependence of inter-band atomic transitions. These interesting properties of graphene like the ability to tune the fermi level by electrical gating, strong optical transitions, etc., are promising for various optoelectronics applications.

**J. Li, *et al.*, in 2008 [41]** presented a systematic procedure for designing flat band photonic crystal waveguide for slow light propagation. In this technique, the first two rows of air-holes in the vicinity of the line-defect are varied from their normal position. This optimization helps to attain a very large value of the group index bandwidth product, which is required to be quite high in photonic crystal waveguide applications.

**Y. Huang, *et al.*, in 2008 [13]** proposed a two dimensional slab of photonic crystal waveguide on silicon on insulator wafer. Band gaps of guided and index guided modes were discussed by measuring the transmission spectra. Imperfections had been considered during the fabrication of structure and all characteristics were investigated. High coupling efficiency and short coupling length were also realized successfully by using suppressive power reservation technique.

**T. Baba, *et al.*, in 2008 [42]** discussed that low group velocity is a promising solution for buffering and time domain processing of optical signals and also discussed various factors to be considered about slow light which involve dispersion compensation and its wide range tunability. He experimentally demonstrated various advancements in the slow-light device technology. He proposed a chirped photonic crystal coupled waveguide on slab fabricated on silicon-on-insulator substrate. He experimentally evaluated a record high value of 57 for the delay-bandwidth product. It indicates the buffering capability of a device and it should be as high as possible. In order to permit variable delays in the device design, he proposed a method for external control of the chirping in the device.

**O. Faolain, et al. in 2009 [43]** designed a low loss slow light photonic crystal with large operating bandwidth. Low loss mechanism has been applied to the device design and loss of about 1 dB/bit was achieved efficiently. They also reported the nonlinear measurements on 80  $\mu\text{m}$  photonic crystal waveguides fabricated from silicon. These types of waveguides are designed for the propagation of dispersion less slow light having very low group velocity. The results highlighted the concept and crucial role of free carrier absorption and two-photon absorption in the photonic crystal waveguides.

**S. Kubo, et al. in 2010 [44]** efficiently achieved high transmission by optimizing the design of two dimensional square lattice of photonic crystal waveguide by introducing line defect in Y shape. Strong coupling is achieved between input and output waveguide by the placement of rods in between for the improvement of transmission coefficients over a wide range of frequencies by further adding the rods in the edge of the output waveguide.

**J. Hou, et al., in 2010 [45]** demonstrated zero-dispersion wideband slow light in a chirped photonic crystal waveguide in coupled configuration. Effects of chirping on a variety of parameters and design principles to achieve the ideal chair shape of the dispersion curve are discussed. The chirping is introduced in the width of photonic crystal waveguide. They numerically established optical confinement of the wideband slow light inside the low dielectric slot region. Proposed structures would possess significant potential for compact high speed optical signal processing devices.

**J. Adachi, et al., in 2010 [46]** demonstrated state-of-the-art slow light in a coupled photonic crystal waveguide. The device design allows the propagation of slow light at a very low group velocity. The technique of structural chirping is utilized to produce tunable delay in the waveguide. This new method of introducing the chirping in the device structure involves applying the concept of folded chirping profile. This idea offers numerous advantages over the conventional way of using monotonous chirping in the waveguide design. Some of the advantages that were elaborately discussed included expansion in the delay tuning range and the suppression of unwanted spectral oscillations. Then considering an unchirped device, they proposed the idea of an index chirping technique which is induced thermally for the purpose of achieving a tunable delay.

**J. Cardenas, et al., in 2010 [47]** demonstrated delay tuning in a device configuration consisting of microring resonators fabricated from silicon. The tuning is induced thermally. A very high value of optical delay equal to 135picoseconds is reported. The design also exhibits a very wide bandwidth of 10 GHz. The key characteristic of this device is very small reported value of group delay dispersion. The device configuration also shows very low losses. The device proposed was compact and easy for on-chip control. Delay tuning in the device is performed with the use of heaters which have been fabricated on top of microrings. It was also observed that in order to enhance the tuning range, the number of microrings can be increased in the device.

**R. Hao, et al, in 2010 [48]** proposed a unique concept of using lattice-shifted photonic crystal waveguides. This type of design optimization helps to increase the group index of slow light propagating in the waveguide. Dispersion can also be reduced to a great extent. The photonic crystal waveguide design is proposed on silicon-on-insulator platform with triangular lattice. This configuration helps in obtaining wideband slow light in the waveguide. It was theoretically discussed that the few rows of holes which are in the vicinity of the waveguide (line-defect) have the most significant impact on the slow light propagating in the waveguide. Therefore, in order to change slow light properties, positions of the rows of air-holes adjacent to the waveguide are carefully altered according to the requirement.

**L. Berman, et al, in 2010 [49]** proposed a unique type of photonic crystal device design using graphene. The photonic crystal was fabricated in a new way by implanting a group of alternating graphene discs and dielectric discs stacks periodically into a background dielectric medium. Theoretically, it was discussed that for far-infrared area of electromagnetic spectrum, graphene-based photonic crystals can find applications as waveguides and frequency filters. Doped graphene is used which helps in reducing absorption of low-frequency radiation. Therefore, the skin effect and damping effect in the photonic crystal were reported to be suppressed. The device structure consisted of a two dimensional photonic crystal. The stacks of graphene discs were placed periodically. These were implanted into the dielectric film. A stack was formed by placing graphene discs on top of each other. These were separated by dielectric placed between them. The dielectric photonic crystals find usage only in the optical region of spectrum. So the idea behind proposing such type of photonic crystal is that these types of devices with the metallic

constituent elements can potentially find usage in the far-infrared region of spectrum. The graphene based photonic crystal device design reported above can be useful at a wide range of temperatures. Various optimizations can be made to the structure to suit the requirement of an application. In order to vary the band structure of this design, thickness of dielectric layers can be changed which are between the graphene discs. The doping of graphene can also be varied according to the requirement.

**C. Charlier, *et al*, in 2010 [50]** reviewed recent advances in the emerging field of graphene based electronics and optoelectronics applications and devices. Graphene offers the possibility of ultra wideband tuning because of the fact that the dispersion of Dirac fermions is linear. It possesses various significant interesting properties like optical transparency, high mobility, stability, flexibility, etc. The real potential of material like graphene can be utilized in optoelectronics and photonics applications. The unique properties of graphene need to be fully exploited. In recent years, graphene has been used in a variety of photonics and optoelectronics applications. Some of the device examples include robust and flexible touch screen panels, ultrafast lasers, light emitting devices, solar cells and photo detectors.

**Rey, *et al*, in 2011 [51]** discussed various phenomena in photonic crystal waveguides which have high potential to be utilized in slow light applications. The effects of four-wave mixing self-phase modulation and two-photon absorption on nonlinear enhancement of slow light were observed. Low-dispersion slow light was reported in the device. The photonic band structure and transmission spectrum were observed. Emphasis was laid on reducing the losses.

**M. Liu, *et al*, in 2011 [27]** experimentally demonstrated a high-speed waveguide integrated broadband electro absorption modulator fabricated using graphene. The modulation was reported over a wide bandwidth from 1.35 to 1.6 $\mu\text{m}$ . Frequencies over 1GHz were also shown to be modulated with the device. Use of graphene helps in reducing the device size. The device size was reported to be 25 $\mu\text{m}^2$ .

**Y. Zhai, *et al*, in 2012 [52]** realized flat-band slow light in ring-shape-hole photonic crystal waveguide by introducing defects in outer and inner radii of holes in ring shape hole photonic crystal waveguide. With appropriate modifications in outer and inner radii, the slow light property could be optimized. Also by introducing the oblique structure the flat

dispersion bandwidth could be obtained and it made the structure considerably potential for optical buffering and signal transmission applications.

**N. Ishikura, *et al.*, in 2012 [53]** fabricated photonic crystal slow light waveguides integrated with multi-heaters. By optimizing heating powers and adjusting the index distribution, a clear delay peak was observed. By adjusting the heating pattern, chirp arising from fabrication errors were compensated for and a delay peak was reported.

**D. Beggs, *et al.*, in 2012 [54]** introduced the concept of indirect photonic transitions. They demonstrated that it can be used to modify the group velocity of an optical signal. Hence they proposed a dynamic delay line based on this concept. The approach was flexible, in a way such that individual pulses in a pulse stream could be controlled independently. This technique is compatible with the conventional silicon chip technology. They also proposed using carrier injection and carrier depletion in the delay line for delay tuning. Hence forth, external laser is not required.

**K. Kondo, *et al.* in 2013 [55]** demonstrated a way to tune the delay of the signal pulse all optically using two types of slow light in the lattice shifted photonic crystal waveguide. Two photon absorption induced carrier plasma effect gives rise to the dynamic tuning, leading to ultrafast delay tuning. It is not limited by the carrier lifetime but by the incident timing of the control pulse and device length. This device could be integrated with heaters and p-n diodes, using a CMOS-compatible process and thus can be used to externally control delay characteristics, target wavelength and dispersion.

**C. Caer, *et al.*, in 2013 [56]** demonstrated ultrafast delay tuning of a slow light pulse with a response time less than 10ps. This is achieved by the using two types of slow light: dispersion-compensated slow light for the signal pulse and low dispersion slow light to enhance nonlinear effects of the control pulse. These two types of slow light are generated simultaneously in silicon lattice-shifted photonic crystal waveguides, arising from flat and straight photonic bands, respectively. The control pulse blue shifts the signal pulse spectrum, through dynamic tuning caused by the plasma effect of two-photon-absorption-induced carriers. This changes the delay by up to 10ps only when the two pulses overlap within the waveguide and enables ultrafast tuning that is not limited by the carrier lifetime.

**R. Hayakawa, *et al.*, in 2013 [57]** proposed and fabricated a new device configuration of photonic crystal waveguides fabricated from silicon to demonstrate high speed delay tuning of slow light. The tuning is controlled electrically. The device consists of an embedded i-region chirped p-i-n diode. By applying a forward bias, carrier plasma effects are generated in the device configuration. The proposed results have high potential to be used in optical signal processing applications.

**F. Weng, *et al.*, in 2013 [26]** reported a significant change in the resonance of a photonic crystal cavity when they gated a graphene layer electrically on top of cavity. Ion gel gating is used in the device for the purpose of electrical gating. An approximate  $\sim 2\text{nm}$  change in cavity resonance line width and about 400% (6dB) change in resonance reflectivity were experimentally reported. This demonstrated that a graphene based photonic crystal device has potential to be used as a low power absorptive/refractive modulator which has high modulation speed and very small physical device size.

**X. Gan, *et al.*, in 2014 [33]** demonstrated modulation of a photonic crystal nano cavity electrically which has an integrated graphene layer. Fermi energy of graphene layer is tuned to 0.85eV. This helps in enhancing optical conductivity at telecommunication wavelength. Large increase in quality factor is reported. Resonance of the cavity undergoes a shift of about 2nm at 1570nm. Choosing various doping levels, conductivity of graphene was determined.

**J. Tang, *et al.*, in 2014 [58]** presented an efficient method to optimize the slow light an ellipse-hole photonic crystal waveguide. The design was studied with finite difference time-domain method. Slow light with large group index and low dispersion is desirable over a wide bandwidth. Various changes can be made to the structure to optimize these parameters.

**X. Gan, *et al.*, in 2014 [33]** proposed that using graphene on planar photonic crystal nanocavities helps to selectively enhance the coupling of light with graphene. A significant enhancement in the absorption of the cavity based device was observed. Various other phenomena like hot photoluminescence and Raman scattering of a graphene layer were elaborately discussed in the proposed design. The usage of graphene in photonic crystal nano-cavity enables enhancement in the light-matter interaction. A transmission attenuation of about 6.2dB was reported over  $70\mu\text{m}$  waveguide length.

**H. Zhou, *et al*, in 2014 [28]** demonstrated enhanced four-wave mixing in a graphene based photonic crystal waveguide. Four-wave mixing conversion efficiency of -23 dB was achieved with this design. Their measurements matched fit with nonlinear coupled-mode theory simulations. This idea proposes an effective way for optical signal processing on chip-scale integrated optics.

**R. Asadi, *et al*, in 2014 [29]** proposed that by increasing of intensity of pump light, refractive index of graphene increases by a large amount due to Kerr nonlinearity, shifting the Fano resonance frequency in the photonic crystal slab. Graphene has high Kerr nonlinearity of about  $n_2=10^{-7}\text{cm}^2/\text{W}$ . This property finds application in phase shifters and phase modulators, optical phase logic devices for optical computations and optical phase shift-keying in communication systems.

**Y. Gong, *et al*, in 2015 [30]** exhibited the tuning characteristics of complex refractive index of graphene. The refractive index was tuned by applying an electric voltage. The reported results matched with the calculations of Kubo formula. The calculation was done for wavelength of 1550 nm.

# Chapter 4

## Electrically Controlled Group Delay in Graphene based Photonic Crystal Waveguide

### 4.1 Methodology of Photonic crystal Modeling

For the modeling of optical structures, a large variety of models are used. On one hand, there exist a number of approximate models that are typically quite fast. However, they have a restricted domain of validity. On the other hand, there is a large class of models where Maxwell's equations are solved exactly, the only approximation being the finite mesh size or the finite number of terms retained in a series expansion. These models tend to be quite slow. One of these methods has been used and is elaborated below.

#### 4.1.1 Wave Equations and Eigen Value Problem

The study of wave propagation in a three-dimensional periodic medium was first undertaken by Felix Bloch. He proved that waves in such a medium can propagate without scattering. The behavior of the waves propagating in periodic media is governed by a periodic envelope function multiplied by a plane wave. He reported that electrons in a conductor scatter only from imperfections. The same techniques can be applied to electromagnetism by casting Maxwell's equations as an Eigen problem in analogue with Schrodinger's equation. Also, Eigen operator is positive-definite and Hermitian. This implies that the Eigen frequencies are real and also leads to orthogonality and perturbation-theory relations. Maxwell equations elaborate the interaction of light with matter. Macroscopic electromagnetism which also includes the propagation of light in a photonic crystal is governed by the four macroscopic Maxwell equations given as [1]

$$\begin{aligned}\nabla \cdot B &= 0 \\ \nabla \cdot D &= \rho \\ \nabla \times E &= -\frac{\partial B}{\partial t} \\ \nabla \times H &= J + \frac{\partial D}{\partial t}\end{aligned}\tag{4.1}$$

where  $\mathbf{E}$  and  $\mathbf{H}$  are the macroscopic electric and magnetic fields,  $\mathbf{D}$  and  $\mathbf{B}$  are the displacement and magnetic induction fields, and  $\mathbf{J}$  and  $\rho$  are the current and free charge densities respectively. Propagation within a mixed dielectric medium consists of composite regions of homogeneous dielectric material. It varies as a function of the Cartesian position vector ' $\mathbf{r}$ ' but the structure does not vary with time and also there are no free charges or currents. For such medium in which light propagates but there are no sources of light, we can set  $\rho = 0$  and  $\mathbf{J} = 0$ . The relative positions of the regions of dielectric material can be described by their position vector  $\vec{\mathbf{r}}$ . We consider the material to be isotropic, non-magnetic and lossless, i.e., a linear material with a real and positive permittivity, and unity permeability that is not dependent upon the frequency of radiation. The relations for  $D(\mathbf{r})$  and  $B(\mathbf{r})$  are then given by:

$$\begin{aligned} \mathbf{D}(\mathbf{r}) &= \epsilon_0 \epsilon(\mathbf{r}) \mathbf{E}(\mathbf{r}) \\ \mathbf{B}(\mathbf{r}) &= \mu_0 \mu(\mathbf{r}) \mathbf{H}(\mathbf{r}) \end{aligned} \quad (4.2)$$

(where  $\mu_0 = 4\pi \times 10^{-7}$  Henry/m is the vacuum permeability) and  $\mathbf{B} = \mu_0 \mathbf{H}$ . With these assumptions, the Maxwell equations become

$$\begin{aligned} \nabla \cdot \mathbf{H}(\mathbf{r}, t) &= 0 \\ \nabla \cdot \mathbf{D} &= \rho \\ \nabla \times \mathbf{E}(\mathbf{r}, t) + \mu_0 \frac{\partial \mathbf{H}(\mathbf{r}, t)}{\partial t} &= 0 \\ \nabla \times \mathbf{H}(\mathbf{r}, t) - \epsilon_0 \epsilon(\mathbf{r}) \frac{\partial \mathbf{E}(\mathbf{r}, t)}{\partial t} &= 0 \end{aligned} \quad (4.3)$$

In general, both  $\mathbf{E}$  and  $\mathbf{H}$  are complicated functions of both time and space. Because the Maxwell equations are linear, we can separate the time dependence from the spatial dependence by expanding the fields into a set of harmonic modes. This allows us to write a harmonic mode as a spatial pattern or mode profile times a complex exponential:

$$\begin{aligned} \mathbf{H}(\mathbf{r}, t) &= \mathbf{H}(\mathbf{r}) e^{-j\omega t} \\ \mathbf{E}(\mathbf{r}, t) &= \mathbf{E}(\mathbf{r}) e^{-j\omega t} \end{aligned} \quad (4.4)$$

To find the equations governing the mode profiles for a given frequency, we insert the above equations (4.4) into (4.3). The two divergence equations give the conditions as

$$\nabla \cdot H(r) = 0$$

$$\nabla \cdot [\epsilon(r)E(r)] = 0 \quad (4.5)$$

which have a simple physical interpretation: there are no point sources or sinks of displacement and magnetic fields in the medium. Equivalently, the field configurations are built up of electromagnetic waves that are transverse. The two curl equations relate  $\mathbf{E}(r)$  to  $\mathbf{H}(r)$  as:

$$\nabla \times E(r) - i\omega\mu_0 H(r) = 0$$

$$\nabla \times H(r) + i\omega\epsilon_0\epsilon(r)E(r) = 0 \quad (4.6)$$

These equations can be decoupled in the following way. First of all divide the bottom equation of (4.6) by  $\epsilon(r)$ , and then take its curl. Then use the first equation to eliminate  $\mathbf{E}(r)$ . The constants  $\epsilon_0$  and  $\mu_0$  can be combined to yield the vacuum speed of light,  $c = 1/\sqrt{\epsilon_0\mu_0}$ .

The result is the **Master Equation** entirely in  $\mathbf{H}(r)$ :

$$\nabla \times \left( \frac{1}{\epsilon(r)} \nabla \times H(r) \right) = \left( \frac{\omega}{c} \right)^2 H(r) \quad (4.7)$$

Together with the divergence equation (4.5), this master equation explains everything about  $\mathbf{H}(r)$ . For a given structure  $\epsilon(r)$ , solve the master equation to find the modes  $\mathbf{H}(r)$  and the corresponding frequencies, by considering transversality condition also. Using the second equation of (4.6) to recover  $\mathbf{E}(r)$ :

$$E(r) = i\omega\epsilon_0\epsilon(r)(\nabla \times H(r)) \quad (4.8)$$

This method ensures that  $\mathbf{E}$  satisfies the transversality requirement  $\nabla \cdot (\epsilon\mathbf{E}) = 0$ , because the divergence of a curl is always zero. Thus, we need to impose only one transversality constraint. The reason why we chose to formulate the problem in terms of  $\mathbf{H}(r)$  and not  $\mathbf{E}(r)$  is merely mathematical convenience. We can also find  $\mathbf{H}$  from  $\mathbf{E}$  via the first equation of (4.6).

$$H(r) = -i\omega\mu_0(\nabla \times E(r)) \quad (4.9)$$

The content of equation (4.7) states that if  $H(r)$  is an allowable electromagnetic mode, the result after the operations of the equation are just a constant times the original function  $H(r)$ .

This is now an Eigen value problem, in which  $H(r)$  is the eigenvector and  $\left(\frac{\omega}{c}\right)^2$  is the Eigen

value. The eigenvectors  $H(r)$  are the field patterns of the harmonic modes in the dielectric material and the Eigen value  $\left(\frac{\omega}{c}\right)^2$  are proportional to the squared frequencies of these modes [1]. It can also be shown that the operator  $\Pi = \nabla \times \left(\frac{1}{\epsilon(r)} \nabla \times\right)$  is linear and Hermitian. A Hermitian operator implies that the Eigen functions (modes of different energies) are orthogonal and have real Eigen value. If two harmonic modes have equal frequencies ( $\omega_1 = \omega_2$ ), then they are degenerate and not essentially orthogonal. A significant property of the electromagnetic modes is that there is no specified length scale involved. Once the Eigen value and Eigen functions of equation (4.7) are solved, they can be scaled to any physical size or wavelength range as long as the dielectric constant is fixed.

#### 4.1.2 Computational Technique – Planewave Expansion method

We used MIT Photonic Bands (MPB) software package to solve numerically the Eigen value problem and determine the band structure of the photonic crystal waveguide. It is a frequency-domain method. It computes Eigen modes with plane wave expansion method [16], which refers to a computational technique in electromagnetics to solve the Maxwell's equations by formulating an Eigen value problem. MPB takes a periodic dielectric structure and computes the Eigen modes of that structure, which are the electromagnetic waves that can propagate through structure with a definite frequency.

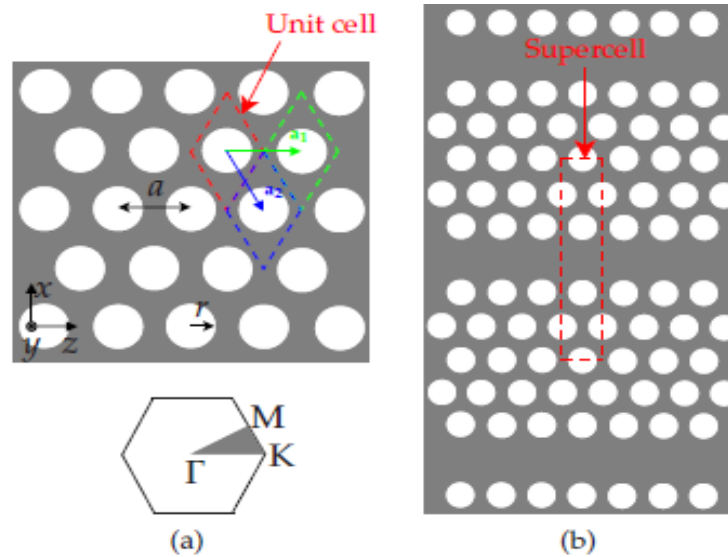


Figure 4.1: (a) Schema of 2d photonic crystal of hexagonal lattice of air holes in high dielectric material. Unit cell is repeated infinitely along the primitive vectors  $a_1$  and  $a_2$ . Its first Brillouin zone, with high symmetry

points, is shown underneath. (b) Two dimensional photonic crystal line-defect waveguide defined by the repetition of a supercell [17].

A photonic crystal has dielectric function which is periodic for the primitive lattice vectors. Bloch-Floquet theorem yields a different Hermitian Eigen problem over primitive cell of lattice at each Bloch wave vector  $k$ . If the structure is periodic in all directions then the primitive cell is finite which leads to discrete Eigen values. Eigen solutions are periodic functions of  $k$ . Due to this periodicity, one need to only compute Eigen solutions for  $k$  within primitive cell of reciprocal lattice or consider the set of inequivalent wavevectors closest to  $k=0$ , a region called first Brillouin zone. First Brillouin zone may itself be redundant if crystal possesses additional symmetries. By the elimination of the redundant regions, the irreducible Brillouin zone is obtained, which is a convex polyhedron. Complete band gap is a range of Eigen values in which there are no propagating solutions of Maxwell's equations for any wavevector  $k$  (i.e., real values of  $k$ ), surrounded above and below the gap by propagating states. Incomplete gaps are also present. Any periodic dielectric variation in one dimension will lead to formation of a band gap, although there is a small gap for a small variation. For a complete band gap to exist in two or three dimensions, additional obstacles must be overcome. Although at each  $k$  point of the crystal, there will be photonic band gap in one-dimension, these gaps will not usually overlap in frequency or lie between the same bands. The band gaps must be adequately large so that they can overlap. If the periodicity is same in different directions, then also large band gap occurs. Therefore, largest band gaps occur in hexagonal lattices in two dimension and fcc lattices in three dimension, which have most nearly circular and spherical Brillouin zones.

## 4.2 Design of Proposed Device

A photonic crystal slab with high refractive index dielectric material (Si) with air-holes arranged in hexagonal array is most attractive photonic crystal structure. A triangular lattice photonic crystal slab consisting of circular air holes ( $n=1$ ) on silicon layer ( $n=3.48$ ) fabricated on a silicon-on-insulator substrate is considered. In such structure light can be confined vertically by total internal reflection. Combining this in-plane confinement with the vertical confinement due to the index contrast in the vertical direction, 3D light confinement is possible within a waveguide in a photonic crystal slab. The waveguide is formed by

introducing line-defect, i.e., by removing the central row of air holes along the x direction. We have considered the slab height as 220 nm. The lattice constant ‘ $a$ ’ is the distance between centers of the holes and it is chosen to be 430 nm for both directions x and y. Air holes with radius  $0.30a$  and refractive index 1 are etched on silicon slab to height 1.001 of slab height. This height is chosen to ensure holes are etched in silicon slab properly. Two designs are proposed: one with graphene layer on the core region (line-defect) and other with graphene layer on the cladding region. The proposed device designs are depicted in Fig. 4.2 a) and b). As discussed earlier, graphene is a two dimensional material whose properties can be efficiently controlled through applied electric voltage, therefore, a graphene based photonic crystal waveguide is proposed in order to control the transmission of light through the waveguide by the use of electric voltage.

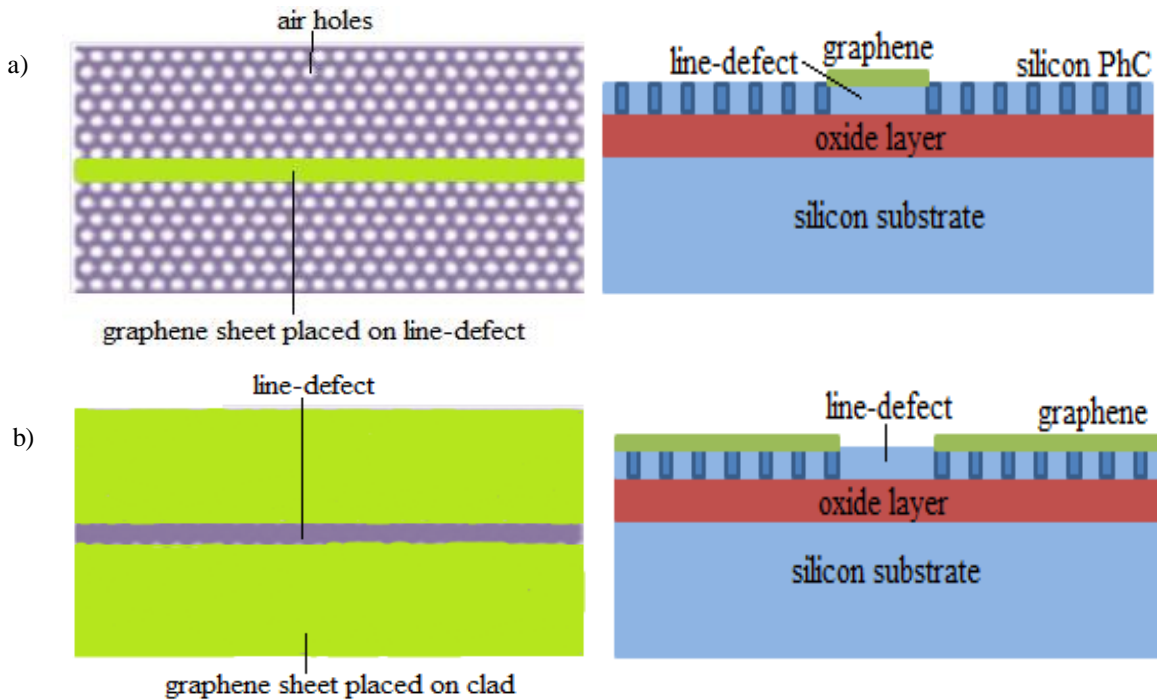


Figure 4.2: a) Top view and cross sectional view of the graphene based photonic crystal waveguide device design in which graphene layer is placed on the core region (line-defect). b) Top view and cross sectional view of the graphene based photonic crystal waveguide device design in which graphene layer is placed on the cladding region. The basic two dimensional photonic crystal is fabricated made on a SOI platform. On silicon substrate, a layer of  $\text{SiO}_2$  is deposited. Over which top silicon layer is present in which air holes ( $n=1$ ) are etched, which provides the required dielectric contrast.

Since a layer of graphene is very thin. Therefore, it will take tremendous computation time in simulations. So, for a practical treatment of it, we replace the graphene layer by an

equivalent composite layer with an equivalent dielectric constant. This helps in making the simulation faster and easier. Also in this way, the band structure and various other profiles can be observed easily in order to observe the light guiding in graphene based photonic crystal waveguide.

### 4.3 Effect of Graphene on Guiding Characteristics

The properties of the proposed device designs are numerically analyzed by using the plane wave expansion method which is suitable to estimate slow light properties of the photonic crystal waveguide. The slab equivalent index method is used by selecting an appropriate supercell. The refractive index of silicon and graphene were used as 3.48 and 1.8 at 1550nm. For the numerical simulation, the supercell selected is shown in figure 4.3. Direction of periodicity considered is along the waveguide (the  $x$ -direction) and all the calculations are made for wave vector range  $0.3 \leq k_x \leq 0.5$ , as this is the region which corresponds to low group velocity.

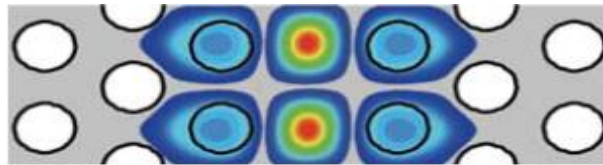


Figure 4.3: Electric field energy density profile of the guided mode in graphene based photonic crystal waveguide calculated by the plane wave expansion method showing the band gap guiding effect.

The line-defect disturbs the periodicity of air-holes which helps in obtaining strong optical confinement in the narrow region. The periodic structure surrounding the defect causes a collective cancellation of scattering of light leading to guiding of light in the defect region. Figure 4.3 shows electric field pattern of guided band. It is the Electric field energy density calculated by plane wave expansion method for the slow light regime. The field localization in the waveguide (centerline) is apparent in the figure 4.3, confirming the band gap guiding effect.

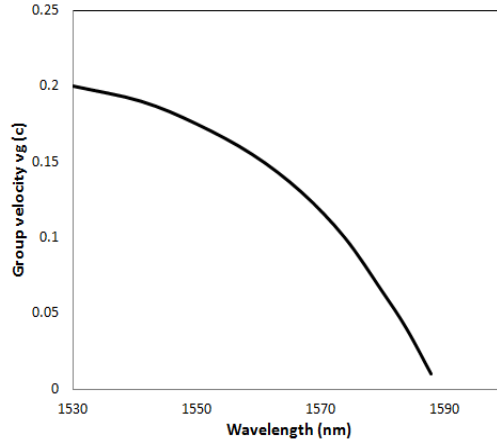


Figure 4.4: Group velocity ( $v_g$ ) of the defect guided mode in the waveguide in the units of  $c$  (the speed of light in the vacuum), for the photonic crystal waveguide without the use of graphene.

Figure 4.4 shows the variation of group velocity  $v_g$  ( $c$ ) with wavelength in the photonic crystal waveguide when graphene is not used. Figure 4.5 a) shows the calculated values of group velocity  $v_g$  ( $c$ ) in the graphene based photonic crystal waveguide when graphene is placed on the core region (line-defect) and b) shows the values of group velocity  $v_g$  ( $c$ ) in the graphene based photonic crystal waveguide when graphene is placed on the cladding region.

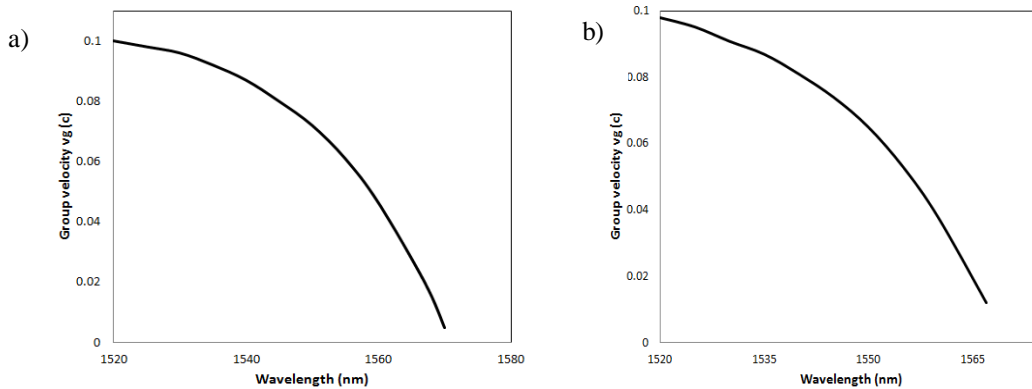


Figure 4.5: Group velocity ( $v_g$ ) of the guided mode in the graphene based photonic crystal waveguide a) when graphene is placed on the core region (line-defect) b) when graphene is placed on the cladding region.

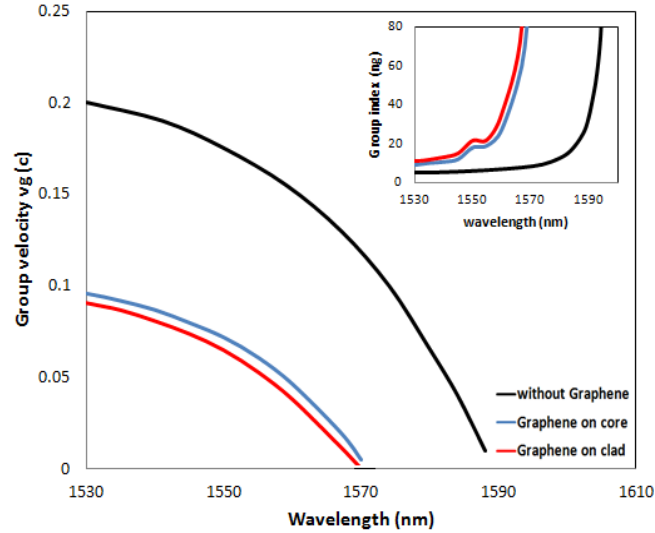


Figure 4.6: Group velocity versus wavelength for photonic crystal waveguide and effect of graphene on core/clad. The inset shows effect of graphene (core/clad) on group index ( $n_g$ ) indicating slow light enhancement.

Figure 4.6 shows variations of group velocity  $v_g$  (c) with wavelength for the PCW without graphene and with graphene on core/clad. In the photonic crystal waveguide without graphene, a group velocity of  $0.1724c$  is obtained at  $1550\text{nm}$ . For the structure with graphene on the core, a group velocity of  $0.0769c$  and for the structure with graphene on the clad, a group velocity of  $0.057c$  is obtained at  $1550\text{ nm}$ . FLG is a semi-metal which can form surface plasmon polariton at the interface of FLG and silicon. The SPP thus formed modifies the optical mode guided in the PCW. The interaction of SPP increases the group index of the guided mode thereby slowing down the light further as shown in the inset of Figure 4.6. A significant reduction in the group velocity is observed in photonic crystal waveguide having graphene as compared to the device without graphene at the telecommunication wavelength. The reduction in group velocity implies increase in group delay ( $\Delta t$ ), which is advantageous for delay tuning applications.

#### 4.4 Electrical control of graphene

In proposed structure, the voltage applied to the device is varied. By change in applied voltage, the optical properties of graphene sheet vary. This implies that there is variation in ‘ $\epsilon$ ’ with changing electric voltage. This causes variation in the group velocity. The variation of group velocity results in a variable group delay of the slow light, propagating through the waveguide and thus delay tuning is achieved in graphene based photonic crystal waveguide.

The real ( $\epsilon'_{\mathbf{g}}$ ) and imaginary ( $\epsilon''_{\mathbf{g}}$ ) part of graphene dielectric constant vary upon electrical gating. These are calculated by [25]

$$\epsilon'_{\mathbf{g}}(E_{\mathbf{f}}) = 1 + \frac{e^2}{8\pi E \epsilon_0 d} \ln \frac{(E + 2|E_{\mathbf{f}}|)^2 + \Gamma^2}{(E - 2|E_{\mathbf{f}}|)^2 + \Gamma^2} - \frac{e^2}{\pi \epsilon_0 d} \frac{|E_{\mathbf{f}}|}{E^2 + (\frac{1}{\tau})^2} \quad (4.1)$$

$$\begin{aligned} \epsilon''_{\mathbf{g}}(E_{\mathbf{f}}) = & \frac{e^2}{4E\epsilon_0 d} \left[ 1 + \frac{1}{\pi} \left\{ \tan^{-1} \frac{E - 2|E_{\mathbf{f}}|}{\Gamma} - \tan^{-1} \frac{E + 2|E_{\mathbf{f}}|}{\Gamma} \right\} \right] \\ & + \frac{e^2}{\pi \tau E \epsilon_0 d} \frac{|E_{\mathbf{f}}|}{E^2 + (\frac{1}{\tau})^2} \end{aligned} \quad (4.2)$$

where  $\Gamma$  is the interband transition broadening. From the graphene reflection spectrum, it is found as 110 meV. Free carrier scattering rate  $1/\tau$  has small effect on the dielectric constant. Therefore, it is taken as zero. Since the waveguide is designed for operation in a narrow bandwidth, it is sufficient to calculate the dielectric constant by using single operating wavelength ( $\lambda = 1550\text{nm}$ ). The Fermi level of graphene ( $E_{\mathbf{f}}$ ) and the applied voltage ( $V$ ) can be related as [25]

$$E_{\mathbf{f}} = \hbar v_{\mathbf{f}} \sqrt{\pi \left( n_0 + \frac{C|V|}{q} \right)} \quad (4.3)$$

where  $C$  is effective capacitance per unit area,  $v_{\mathbf{f}} \sim 10^6$  m/s is Fermi velocity for graphene, and  $n_0$  is intrinsic carrier concentration. Effective capacitance of ion gel gating  $C \sim 20$  mF/m<sup>2</sup> and any intrinsic carrier concentrations are neglected.

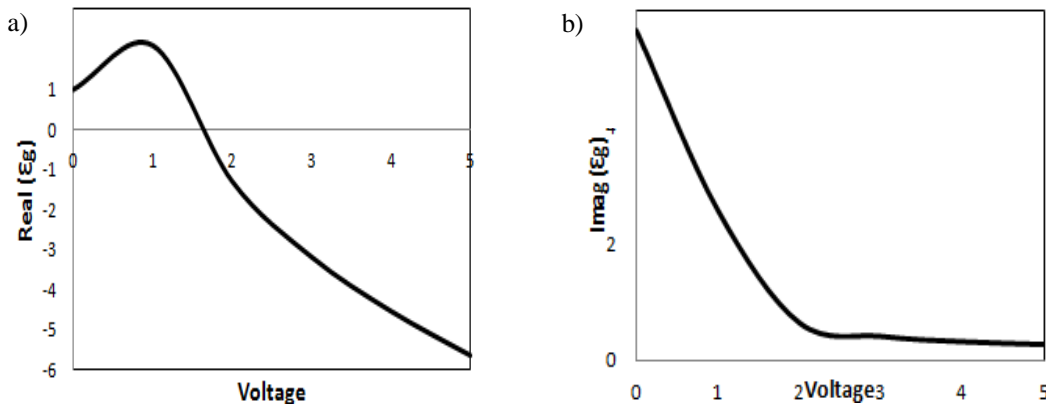


Fig 4.7: The real and imaginary part of the dielectric constant of graphene as a function of the applied gate voltage. The real part is a non-monotonic function of the applied voltage. The imaginary part decreases monotonically with increasing voltage.

$\epsilon_g'$  has significant contribution both from intraband and interband transitions. It is observed that the imaginary part of  $\epsilon_g(\omega)$ , which is responsible for the light absorption, decreases monotonically with increasing voltage, especially when the  $2|E_F|$  is larger than the resonance energy  $E_r$ . On the other hand, the real part of  $\epsilon_g(\omega)$  is a non-monotonic function of the applied voltage which is depicted in Figure 4.7. The change in the dielectric constant with applied voltage helps in the modification of the parameters of the guided mode propagating through the graphene based photonic crystal waveguide.

## 4.5 Delay Tuning

The observed tunability of the complex reflective index as the function of gate electric voltage is in agreement with the prediction based on the Kubo formula. First of all, we determined the group velocity variation in the photonic crystal waveguide with the applied electric voltage when graphene is not used. A large group velocity variation can be observed but with the drawback of very large electric voltage requirement. Therefore, wide delay tuning can be observed only with large amount of applied electric voltage which is not suitable for on-chip delay tuning applications. Figure 4.8 shows the variation in group velocity with change in applied voltage.

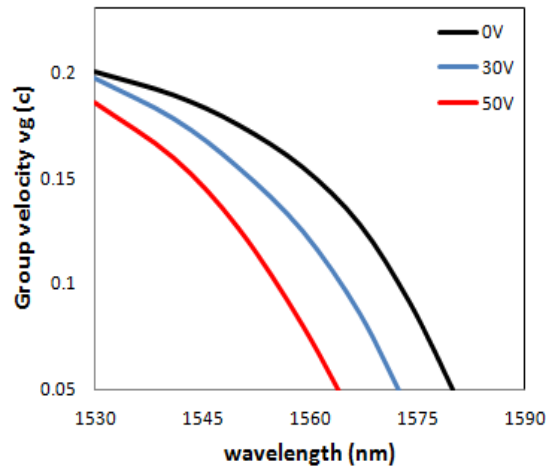


Figure 4.8: The variation of Group velocity of the guided mode in photonic crystal waveguide with applied electric voltage. Here black line denotes no voltage, blue line indicates 30V and red line indicates group velocity when 50V is applied to the device.

As shown in figure 4.8, with increase in applied electric voltage, a reduction in group velocity is reported. Therefore, with reduction in group velocity, there is subsequent increase

in the group delay. With no applied voltage at wavelength 1550nm a group velocity value of 0.17c is reported. With an applied voltage of 30V, group velocity of 0.1c is observed and therefore a group delay value of 33.4 picoseconds is reported. With an applied voltage of 50V, group velocity of 0.08c is observed and thus a group delay value of 66.7 picoseconds is reported at wavelength of 1550nm. Figure 4.9 shows the variation of group delay with the applied voltage for photonic crystal waveguide at telecommunication wavelength (1550nm) when graphene is not used in the device structure. It is clearly observed that obtaining high values of group delay requires application of very large amount of electric voltage which is not suitable in practical delay-tuning applications.

For our wavelength of interest, i.e., 1550 nm, group velocity is tuned from 0.1769c to 0.054c with 50 volts of electric voltage applied. Hence the group delay is tuned from 33.4 picoseconds to 66.7 picoseconds. With application of electric voltage, change in value of group delay is observed at 1550nm. With increasing voltage, value of group delay increases.

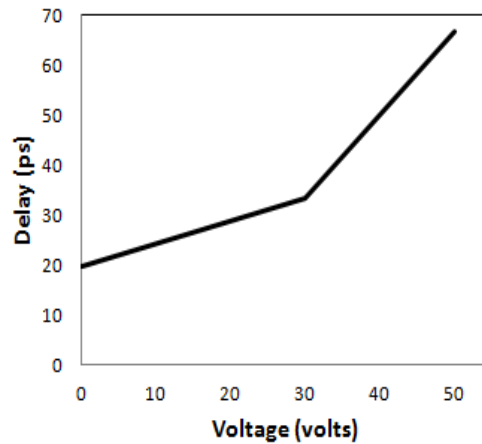


Figure 4.9: Tunable Delay (in picoseconds) of the Photonic crystal waveguide without using graphene at 1550nm. This depicts that with increasing voltage, group delay increases.

Now proceeding with our analysis of graphene based photonic crystal waveguide, we determined the group velocity variation in the graphene based photonic crystal waveguide with the applied electric voltage when graphene is placed on the core. A large group velocity variation can be observed with very low electric voltage requirement. Therefore, wide delay tuning can be observed with very low electric voltage which is suitable for on-chip delay tuning applications. Figure 4.10 shows the reported variation in the group velocity of the device with change in applied voltage. It is apparent from the figure that applying electric

field results in the wavelength shift of the group velocity curve to smaller wavelengths.

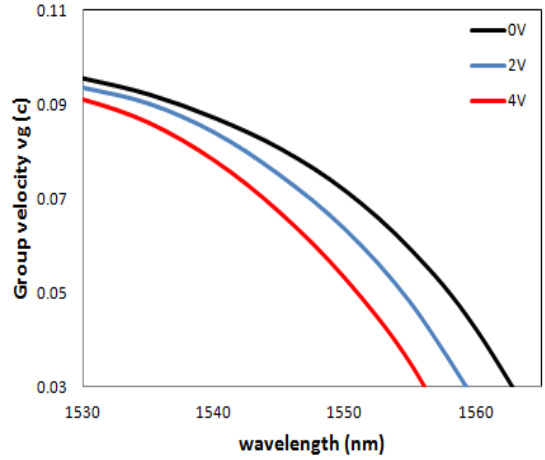


Figure 4.10: The variation of Group velocity of the guided mode in graphene based photonic crystal waveguide with applied electric voltage when graphene is placed on core (line-defect).

With increase in applied electric voltage, a reduction in group velocity is reported. Therefore, there is subsequent increase in the group delay. With no applied voltage at wavelength 1550nm a group velocity value of 0.0769c is reported. With an applied voltage of 2V, group velocity of 0.0625c is observed and therefore a group delay value of 53.34 picoseconds is reported. With an applied voltage of 4V, group velocity of 0.0464c is observed and thus a group delay value of 71.83 picoseconds is reported at wavelength of 1550nm.

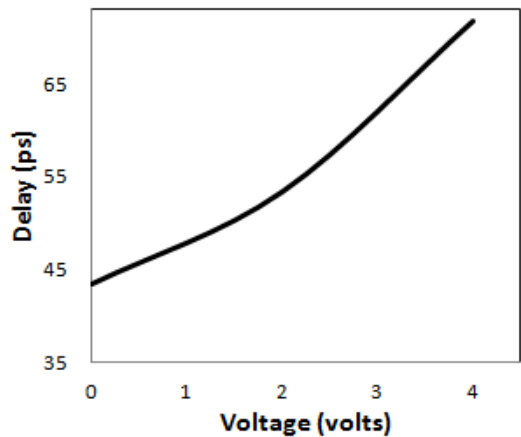


Figure 4.11: Tunable Delay (in picoseconds) of the graphene based photonic crystal waveguide at 1550nm when graphene is placed on the core region (line-defect).

Figure 4.11 shows the variation of group delay with the applied voltage for graphene based photonic crystal waveguide at 1550nm when graphene is placed on the core in the device structure. It is clearly observed that high values of group delay can be obtained with

application of very low electric voltage which is suitable for practical on-chip delay-tuning applications. For our wavelength of interest, i.e., 1550 nm, the group velocity is tuned from 0.0769c to 0.0464c with 4volts of electric voltage applied. Hence the group delay is tuned from 43.34 ps to 71.83 ps in our device structure. With application of electric voltage, change in value of group delay is observed at 1550nm. A wide tuning range of 29 picoseconds is reported with this device design.

Now for the second device design we determined the group velocity variation in the graphene based photonic crystal waveguide with the applied electric voltage when graphene is placed on the cladding region, i.e., on the air holes. In this device design as well, a large group velocity variation is reported with very low applied electric voltage. Therefore, wide delay tuning can be achieved with very low electric voltage which is suitable for on-chip delay tuning applications. Figure 4.12 shows the reported variation in the group velocity of the device with change in applied voltage. It is apparent from the figure that applying electric field results in the wavelength shift of the group velocity curve to smaller wavelengths.

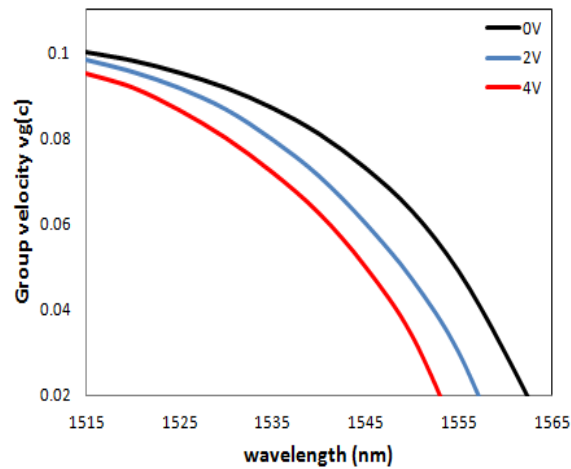


Figure 4.12: The variation of Group velocity of the guided mode in graphene based photonic crystal waveguide with applied electric voltage when graphene is placed on the clad (air-holes).

With increase in applied electric voltage, a reduction in group velocity is reported. Therefore, with reduction in group velocity, there is subsequent increase in the group delay. With no applied voltage at wavelength 1550nm a group velocity value of 0.057c is reported. With an applied voltage of 2V, group velocity of 0.045c is observed and therefore a group delay value of 73.4 picoseconds is reported. With an applied voltage of 4V, group velocity of 0.038c is

observed and thus a group delay value of 86.7 picoseconds is reported at 1550nm.

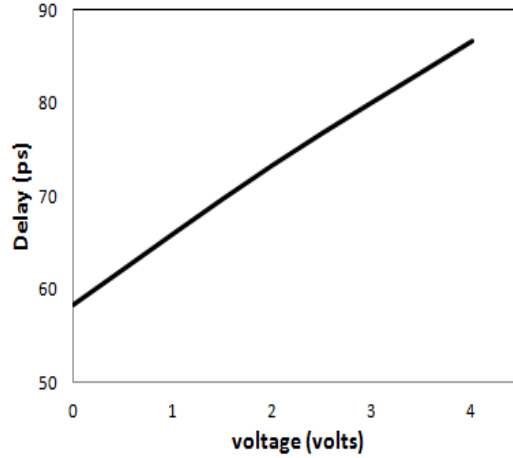


Figure 4.13: Tunable Delay (in picoseconds) of the graphene based photonic crystal waveguide at 1550nm when graphene is placed on the clad (region with air-holes).

Figure 4.13 shows variation of group delay with applied voltage for graphene based photonic crystal waveguide at 1550nm when graphene is placed on the clad. High values of group delay can be obtained with application of very low electric voltage which is suitable for practical on-chip delay-tuning applications. For our wavelength of interest, i.e., 1550 nm, the group velocity is tuned from  $0.057c$  to  $0.038c$  with 4volts of electric voltage applied. Hence the group delay is tuned from 58.4 picoseconds to 86.7 picoseconds. A wide tuning range of 29 picoseconds is reported with this device design.

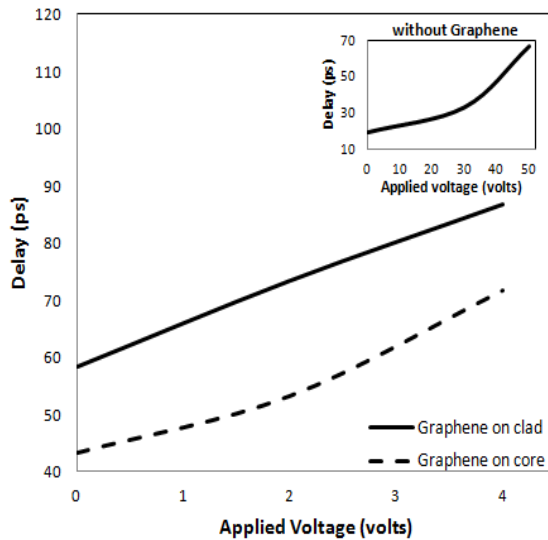


Fig 4.14: Comparison of tuning of group delay by varying applied voltage on graphene (on core/clad) at a wavelength of 1550 nm. The inset shows the delay vs. applied voltage for the PCW without the use of graphene.

Fig. 4.14 compares tuning in group delay of PCW by applying voltage on graphene on core and on cladding of waveguide. We are able to widely tune the delay of the PCW by applying a low voltage on graphene. For the device structure without graphene, group delay as large as 66.7 picoseconds is reported. But attaining high values of the delay in the device requires application of very large amount of electric voltage as high as 50V. Therefore, it will not be feasible for practical on-chip tunable delay applications. On the other hand, similar high values of group delay can be observed in the device structure having graphene with very little amount of voltage applied because Fermi energy of graphene can be tuned considerably with relatively low electric voltage. Therefore, graphene based device design is suitable for low-power applications. Also, a considerable increase in the group delay is reported with the use of graphene. As shown in figure 4.15, group delay of 71.83 picoseconds is obtained with graphene layer on core. For our wavelength of interest, i.e., 1550 nm, group velocity is tuned from  $0.0769c$  to  $0.0464c$  with 4 volts of electric voltage applied. Hence the group delay in the device is tuned from 43.34 picoseconds to 71.83 picoseconds in the device with graphene on core (line-defect). It is also observed that with increasing voltage, group delay also increases. For the device design with graphene on the clad, further increase in group delay is reported. A high group delay value of 86.7 picoseconds is observed. At 1550 nm, group velocity is tuned from  $0.057c$  to  $0.038c$  with 4volts of electric voltage applied. Hence the group delay is tuned from 58.4 picoseconds to 86.7 picoseconds in the device with graphene on the clad. A tuning range of 29 picoseconds is reported with both the device designs. Therefore, graphene based photonic crystal waveguide provides electrically tunable group delay with low power. This design has high potential for on-chip delay tuning applications.

# Chapter 5

## Conclusion and Future Scope

### 5.1 Conclusion

An electrically tunable graphene based photonic crystal waveguide is proposed for delay tuning applications. This dissertation aims to achieve tuning of optical delay in a graphene based photonic crystal waveguide by the application of electric field. A simple approach of tuning the delay is considered on an easy-to-fabricate photonic crystal waveguide without increasing the complexity of the structure. The photonic crystal waveguide structure is first analyzed without graphene and the group velocity variation with electric voltage is observed. The major drawback of using silicon as a photonic material is the low electro optic coefficient. Thus, very small variation in refractive index of silicon is observed with large applied electric voltage. Therefore, large variation in delay is observed only with very large application of electric field voltage as high as 50 volts, which is not suitable for practical delay tuning applications. Therefore, the photonic crystal waveguide structure is analyzed with graphene. The use of few layer graphene is shown to enhance the slow light effect of photonic crystal waveguide. Graphene forms surface plasmon polariton with the guided mode in the photonic crystal waveguide which increases group index of the guided mode. The resulting effect further slows down the light. The Fermi level of graphene can be tuned considerably with low electrical energy, which in turn changes the refractive index of graphene. Thus, presence of graphene not only provides the way to electrically tune the delay with low-power but it also enhances the group delay. Two designs are proposed: one with graphene on the core region (line-defect) and other with graphene on the cladding region. At telecommunication wavelength, i.e., 1550 nm, the group delay is tuned from 43 picoseconds to 72 picoseconds in the first design and from 58 picoseconds to 87 picoseconds in the second device design on varying the applied voltage (on graphene) from 1 volt to 4 volts. A tuning range of 29 picoseconds is observed with both the device designs. Graphene based photonic crystal waveguide can potentially be useful for low-power electrically controllable on-chip delay tuning applications while maintaining a small physical footprint.

## 5.2 Future Scope

In the proposed graphene based photonic crystal waveguide for delay tuning applications, it is possible to further slow down the light by optimizing the photonic crystal waveguide design. Various optimizations can be made to the device structure such as shifting the rows of air-holes adjacent to the line-defect, changing lattice constant, slab width, etc. Thus, values of delay can be improved. Therefore, further enhancement of the delay simply depends on improved structure design. It will help in increasing the delay tuning range which is beneficial for delay line applications. The delay resolution can also be enhanced. Also effort can be made to achieve flat band near  $1.55\mu\text{m}$  because as bandwidth increases buffering capability also increases. Handling the optical delay can be of real interest provided that the delay is tuned with continuity over a wide range and by means of simple, easily-manageable and cost-effective devices. So, the integration of graphene with nano photonic architectures like photonic crystal waveguides has tremendous potential for compact, energy efficient and ultrafast graphene devices for on-chip optical communication and optical interconnects.

## REFERENCES

- [1] Joannopoulos J.D., Meade R.D. and Winn J.N., “Photonic Crystals – Moulding the Flow of Light”, Princeton University Press, Princeton, 1995.
- [2] Noda S., Imada M., Okano M., Ogawa, S., Mochizuki, M., Chutinan A., “Semiconductor three-dimensional and two-dimensional photonic crystals and devices”, *IEEE Journal of Quantum Electronics*, vol.**38**, no.7, pp.726-735, 2002.
- [3] Shanhui, F., Yanik, M.F., Zheng W., Sandhu, S., Povinelli, M.L., “Advances in Theory of Photonic Crystals”, *Journal of Lightwave Technology*, vol.**24**, no.12, pp.4493-4501, 2006.
- [4] Noda S., “Recent Progresses and Future Prospects of Two- and Three-Dimensional Photonic Crystals”, *Journal of Lightwave Technology*, vol.**24**, no.12, pp.4554-4567, 2006.
- [5] Notomi, M., Yamada, K., Shinya, A., Takahashi, C., Yokohama, “Extremely Large Group-Velocity Dispersion of Line-Defect Waveguides in Photonic Crystal Slabs”, *Physical Review Letters*, vol.**87**, no. 25, 2001.
- [6] Baba, T., “Light propagation characteristics of straight single line defect optical waveguides in a photonic crystal slab fabricated into a silicon-on-insulator substrate”, *IEEE J. Quant. Electron.*, vol. **38**, pp.743–752, 2002.
- [7] L. Frandsen, A. Lavrinenko, J. Pedersen, and P. Borel, “Photonic crystal waveguides with semi-slow light and tailored dispersion properties”, *Opt. Express*, vol. **14**, pp. 9444-9450, 2006.
- [8] Kubo, S., Mori, D. and Baba, T., “Low-group-velocity and low-dispersion slow light in photonic crystal waveguides”, *Opt. Lett.*, vol. **32**, pp. 2981–2983, 2007.
- [9] L. Faolain, T. White, D. O'Brien, X. Yuan, M. Settle, and T. Krauss, “Dependence of extrinsic loss on group velocity in photonic crystal waveguides”, *Opt. Express*, vol.**15**, pp. 13129-13138, 2007.
- [10] Vlasov, A., O’Boyle, M., Hamann, H. F. and McNab, S. J., “Active control of slow light on a chip with photonic crystal waveguides”, *Nature*, **438**, pp.65–69, 2005.
- [11] J. E. Sharping, Y. Okawachi, and A. L. Gaeta, “Wide bandwidth slow light using a Raman fiber amplifier”, *Opt. Express*, vol. **13**, pp. 6092, 2005.
- [12] Baba T., “Slow light in photonic crystals”, Review article, *Nature*, vol.**2**, pp.465-473, 2008.

- [13] Yidong Huang, Xiaoyu Mao, Chao Zhang, Lei Cao, Kaiyu Cui, Wei Zhang, and Jiande Peng, “Photonic crystal waveguides and their applications”, *Optics Letters*, vol. **6**, no. 10, pp. 704-708, 2008.
- [14] A. Melloni, A. Canciamilla, C. Ferrari, F. Morichetti, L. O’Faolain, T.F. Krauss, A. Samarelli, M. Sorel, “Tunable Delay Lines in Silicon Photonics: Coupled Resonators and Photonic Crystals, a Comparison”, *IEEE Photonics Journal*, vol. **2**, no. 2, pp. 181-194, 2010.
- [15] J. A. Schuller, E. S. Barnard, W. Cai, Y. C. Jun, J. S. White and M. L. Brongersma, “Plasmonics for extreme light concentration and manipulation”, *Nat. Mater.*, **9**, 193–204, 2010.
- [16] S.G. Johnson & J.D. Joannopoulos, “Block-iterative frequency-domain methods for Maxwell’s equations in a plane wave basis”, *Opt. Express*, **8**, 173-190, 2001.
- [17] Y. Guo, “Simple plane wave implementation for photonic crystal calculations”, *Opt. Exp.*, vol. **11**, pp. 167–175, 2003.
- [18][Online].Available: [http://abinitio.mit.edu/wiki/index.php/MIT\\_Photonic\\_Bands](http://abinitio.mit.edu/wiki/index.php/MIT_Photonic_Bands).
- [19] A.K. Geim and K.S. Novoselov, “The rise of Graphene”, *Nature Mater.*, Vol. **6**, 2007.
- [20] Feng Wang, Yuanbo Zhang, Chuanshan Tian, Alex Zettl, Michael Crommie & Y. Ron Shen, “Gate-Variable Optical Transitions in Graphene”, *Science mag.*, vol.**320**, pp 206, 2008.
- [21] Stauber, T., N. Peres, and A.K. Geim, “Optical conductivity of graphene in the visible region of the spectrum”, *Physical Review B*, vol. **78**, pp. 085432, 2008.
- [22] M. Nakamura and L. Hirasawa, “Electric transport and magnetic properties in multilayer graphene”, *Physical Review B*, vol. **77**, pp. 045429, 2008.
- [23] Bruna, M. and S. Borini, “Optical constants of graphene layers in the visible range”, *Applied Physics Letters*, vol. **94**(3), pp. 031901-3, 2009.
- [24] J. M. Dawlaty, “Measurement of the optical absorption spectra of epitaxial graphene from terahertz to visible”, *Appl. Phys. Lett.*, **93**, 131905, 2008.
- [25] Gusynin, V. P.; Sharapov, S. G.; Carbotte, J. P., “Sum rules for the optical and Hall conductivity in Graphene”, *Phys. Rev. B*, **75**, 165407, 2007.
- [26] Arka Majumdar, Jonghwan Kim, Jelena Vuckovic and Feng Wang, “Electrical Control of Silicon Photonic Crystal Cavity by Graphene”, *Nano Lett.*, vol. **13**, pp. 515–518, 2013.
- [27] Ming Liu, Xiaobo Yin, Baisong Geng, Thomas Zentgraf, Long Ju, Feng Wang & Xiang Zhang, “A Graphene-based broadband optical modulator”, *Nature*, Vol. **474**, 2011.

- [28] Hao Zhou, Tingyi Gu, James F. McMillan, Nicholas Petrone, James C. Hone, Mingbin Yu, Guoqiang Lo, Dim-Lee Kwong, Guoying Feng, Shouhuan Zhou, and Chee Wei Wong, “Enhanced four-wave mixing in graphene-silicon slow-light photonic crystal waveguides”, *Applied Physics Letters*, **105**, 091111, 2014.
- [29] Reza Asadi, Zhengbiao Ouyang, Quanqiang Yu, and Shuangchen Ruan, “All-optical sensitive phase shifting based on nonlinear out-of-plane coupling through 1-D slab photonic crystal with a layer of Graphene”, *Optics express*, Vol. **22**, No. 12, 2014.
- [30] F. Xu, S. Das, Y. Gong, Q. Liu, Y. Chiu, J. Wu, and R. Hui, “Complex refractive index tunability of graphene at 1550 nm wavelength”, *Applied Physics Letters*, **106**, pp-031109, 2015.
- [31] Arka Majumdar, Jonghwan Kim, Jelena Vuckovic and Feng Wang, “Graphene for Tunable Nanophotonic Resonators”, *IEEE Journal of Quantum electronics*, vol. **20**, 2014.
- [32] Jonghwan Kim, Hyungmok Son, David J. Cho, Baisong Geng, Will Regan, Sufei Shi, Kwanpyo Kim, Alex Zettl, Yuen-Ron Shen and Feng Wang, “Electrical Control of Optical Plasmon Resonance with Graphene”, *Nano Letters*, **12**, 5598–5602, 2012.
- [33] Xuetao Gan, Yuanda Gao, Solomon Assefa, James Hone and Dirk Englund, “Controlled Light–Matter Interaction in Graphene Electro optic Devices Using Nano photonic Cavities and Waveguides”, *IEEE Journ. Of Sel. Top. in Quant. Electron.*, Vol. **20**, No. 1, 2014.
- [34] G. Cocorullo and I. Rendina, “Thermo-optical modulator at 1.5  $\mu\text{m}$  in silicon etalon”, *Electron. Lett.*, vol. **28**, no. 1, 1992.
- [35] B. E. A. Saleh, Malvin Carl Teich, “Fundamentals of Photonics”, John Wiley & Sons, Inc. ISBNs: 0-471-2-1374-8, 697-735, 1991.
- [36] R. A. Soref and B. R. Bennett, “Electrooptical effects in Silicon”, *IEEE Journal of Quantum Electronics*, vol. QE-**23**, pp.123-129, 1987.
- [37] N. Moll, G. L Bona, “Comparison of three-dimensional photonic crystal slab waveguides with two-dimensional photonic crystal waveguides: Efficient butt coupling into photonic crystal waveguides”, *Journal of Applied Physics*, vol. **93**, no. 9, pp. 4986-4991, 2003.
- [38] C. Barrios, V. Almeida, “Electro optic Modulation of Silicon-on-Insulator Sub micrometer Size Waveguide Devices”, *Journal of Lightwave Technology*, Vol. **21**, 10, pp. 2332-2339, 2003.

- [39] D. Ohnishi, K. Sakai, M. Imada, and S. Noda, “Continuous wave operation of surface emitting two-dimensional photonic crystal laser”, *Electron. Lett.*, vol. **39**, pp. 612–614, 2006.
- [40] Fengnian Xia, Lidija Sekaric, and Yurii Vlasov, “Ultra-compact optical buffers on a silicon chip”, *Nature Photonics*, vol. **1**, pp. 65–71, 2006.
- [41] J. Li, T. White, L. O’Faolain, A. Gomez-Iglesias, and T. Krauss, “Systematic design of flat band slow light in photonic crystal waveguides”, *Opt. Express*, vol. **16**, pp. 6227-6232, 2008.
- [42] T. Baba, T. Kawasaki, H. Sasaki, J. Adachi, D. Mori, “Large delay-bandwidth product and tuning of slow light pulse in photonic crystal coupled waveguide”, *Opt. Express*, **16**, 9245, 2008.
- [43] Monat C., Corcoran B., Heidari M., Grillet C., White Thomas P., O’Faolain L., Krauss T.F., “Slow light enhancement of nonlinear effects in silicon engineered photonic crystal waveguides”, *Journal of optics express*, vol.**17**, no. 4, pp.2944-2953, 2009.
- [44] Y. Hamachi, S. Kubo, and T. Baba, “Slow light with low dispersion and nonlinear enhancement in lattice-shifted photonic crystal waveguide”, *Opt. Lett.*, **34**, pp. 1072-1074, 2010.
- [45] J. Hou, H. Wu, D. Citrin, W. Mo, D. Gao, and Z. Zhou, “Wideband slow light in chirped slot photonic-crystal coupled waveguides”, *Opt. Express*, vol. **18**, pp. 10567-10580, 2010.
- [46] J. Adachi, N. Ishikura, H. Sasaki, and T. Baba, “Wide Range Tuning of Slow Light Pulse in SOI Photonic Crystal Coupled Waveguide via Folded Chirping”, *IEEE Journal of Quantum Electron.*, vol.**16**, pp. 192, 2010.
- [47] J. Cardenas, M. A. Foster, N. Sherwood-Droz, C. B. Poitras, H. L. R. Lira, B. Zhang, A. L. Gaeta, J. B. Kurgin, P. Morton, and M. Lipson, “Wide-bandwidth continuously tunable optical delay line using silicon microring resonators”, *Opt. Express*, **18**, pp-26525, 2010.
- [48] Ran Hao, E. Cassan, H. Kurt, Jin Hou, X. Le roux, D. Morini, L. Vivien, Dingshan Gao, Zhiping Zhou, and Xinliang Zhang, “Novel Kind of Semi slow Light Photonic Crystal Waveguides With Large Delay-Bandwidth Product”, *IEEE Photonics Technology Letters*, vol. **22**, no. 11, pp. 844-846, 2010.
- [49] Oleg L. Berman, Vladimir S. Boykova, Roman Ya., A. Kolesnikov, Yurii E. Lozovik, “Graphene-based photonic crystal”, *Physics Letters*, **374**, 2010.

- [50] S. Dubois, Z. Zanolli, X. Declerck and C. Charlier, “Electronic properties and quantum transport in Graphene-based nanostructures”, *The European Physical Journal B*, vol. **72**, no. 1, pp. 1–24, 2010.
- [51] D. M. Beggs, I. H. Rey, T. Kampfrath, N. Rotenberg, L. Kuipers, and T. F. Krauss, “Ultrafast Tunable Optical Delay Line Based on Indirect Photonic Transitions”, *Phys. Rev. Lett.* **108**, pp. 213901, 2012.
- [52] Yi Zhai, Huiping Tian, Yuefeng Ji, “Slow Light Property Improvement and Optical Buffer Capability in Ring-Shape-Hole Photonic Crystal Waveguide”, *Journal of Lightwave Technology*, vol.**29**, no.20, pp.3083-3090, 2012.
- [53] M. Shinkawa, N. Ishikura, Y. Hama, K. Suzuki, and T. Baba, “Nonlinear enhancement in photonic crystal slow light waveguides fabricated using CMOS-compatible process”, *Opt. Express*, vol. **19**, pp. 22208, 2012.
- [54] D. M. Beggs, I. H. Rey, T. Kampfrath, N. Rotenberg, L. Kuipers, and T. F. Krauss, “Ultrafast Tunable Optical Delay Line Based on Indirect Photonic Transitions”, *Phys. Rev. Lett.* **108**, pp. 213901, 2012.
- [55] K. Kondo, M. Shinkawa, Y. Hamachi, Y. Saito, Y. Arita, and T. Baba, “Ultrafast Slow Light Tuning Beyond the Carrier Lifetime Using Photonic Crystal Waveguides”, *Phys. Rev. Lett.*, **110**, pp. 053902, 2013.
- [56] C. Caer, X. L. Roux, S. Serna, W. Zhang, L. Vivien, and E. Cassan, “Large group index bandwidth product empty core slow light photonic crystal waveguides for hybrid silicon photonics”, *Frontiers of Optoelectronics*, 2013.
- [57] R. Hayakawa, N. Ishikura, H. C. Nguyen, and T. Baba, “High-speed delay tuning of slow light in pin-diode-incorporated photonic crystal waveguide”, *Optics let.*, Vol. **38**, No. 15, pp 2680-2682, 2013.
- [58] J. Tang, T. Wang, B. Liu, B. Wang and Y. He, “Systematic design of wideband slow light in ellipse-hole photonic crystal waveguides”, *J. Opt. Soc. Am. B*, vol. **31**, pp. 1011-1017, 2014.
- [59] M. Kumar, T. Sakaguchi, and F. Koyama, “Polarization-Insensitive and Low-Loss 3-D Nanostep Hollow Waveguide for Widely Tunable Photonic Devices”, *Journal of Lightwave Technology*, Vol. **26**, 11, pp. 1417-1422, 2008.

- [60] M. Kumar, T. Sakaguchi and F. Koyama, “Tunable Three-Dimensional Nanostep Hollow Optical Waveguide with Low Polarization Dependence”, *Appl. Phys. Express*, **1**, 052002, 2008.
- [61] A. Sharma and M. Kumar, “Flat band slow light in silicon photonic crystal waveguide with large delay bandwidth product and low group velocity dispersion”, *IET Optoelectronics*, Vol. **9**, 1, pp. 24-28, 2015.
- [62] H. Kurt, K. Ustun, and L. Ayas, “Study of different spectral regions and delay bandwidth relation in slow light photonic crystal waveguides”, *Opt. Express*, **18**, pp. 26965-26977, 2010.
- [63] R. Hao, E. Cassan, X. Le Roux, D. Gao, V. Do Khanh, L. Vivien, D. Marris-Morini, and X. Zhang, “Improvement of delay-bandwidth product in photonic crystal slow light waveguides”, *Opt. Express*, vol.**18**, pp. 16309-16319, 2010.
- [64] N. Ishikura, R. Hayakawa, R. Hosoi, M. Shinkawa, T. Baba, “Photonic crystal tunable slow light device integrated with multi-heaters”, *Appl. Phys. Lett.*, Vol. **100**, pp. 221110, 2012.
- [65] Jian Tang, Tao Wang, Xiaoming Li, Boyun Wang, Chuanbo Dong, Lei Gao, Bo Liu, Yu He, and Wei Yan, “Wideband and Low Dispersion Slow light in Lattice-Shifted Photonic Crystal Waveguides”, *J. Lightwave Tech.*, Vol. **31**, No. 19, 2013.

## **PUBLICATIONS**

1. Jobanpreet kaur Thind, Dr. Mukesh Kumar and Dr. Brajesh Kumar Kaushik, “Electrical Tuning of Optical Delay in Graphene based Photonic Crystal Waveguide”, submitted to IEEE Journal of Quantum Electronics, June 2015.